Tailoring graphene electronic properties *via* adsorption of hydrogen atoms

Rocco Martinazzo

Department of Physical Chemistry and Electrochemistry
Universita' degli Studi di Milano, Milan, Italy

Universität Duisburg-Essen
November, 10th 2009

Outline

Outline

Outline

Outline

Technology

- Hydrogen storage
- Nuclear fusion
- Nanoelectronics, spintronics, nanomagnetism

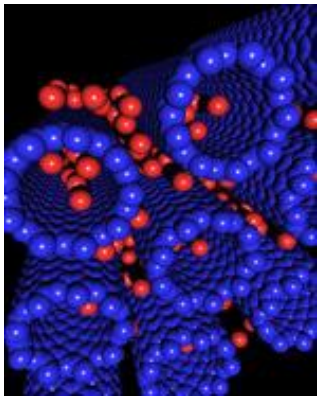

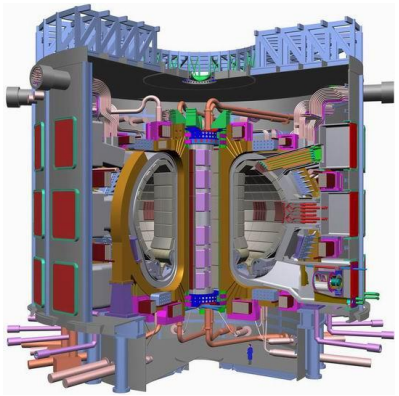

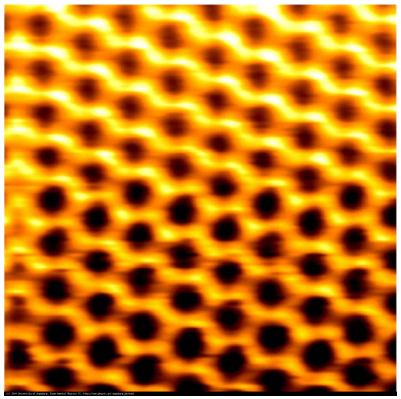

Technology

Electric Field Effect in Atomically Thin Carbon Films

K. S. Novoselov,[1] A. K. Geim,[1]* S. V. Morozov,[2] D. Jiang,[1] Y. Zhang,[1] S. V. Dubonos,[2] I. V. Grigorieva,[1] A. A. Firsov[2]

We describe monocrystalline graphitic films, which are a few atoms thick but are nonetheless stable under ambient conditions, metallic, and of remarkably high quality. The films are found to be a two-dimensional semimetal with a tiny overlap between valence and conductance bands, and they exhibit a strong ambipolar electric field effect such that electrons and holes in concentrations up to 10^{13} per square centimeter and with room-temperature mobilities of ~10,000 square centimeters per volt-second can be induced by applying gate voltage.

The ability to control electronic properties of a material by externally applied voltage is at the heart of modern electronics. In many cases, it is the electric field effect that allows one to vary the carrier concentration in a semiconductor device and, consequently, change an electric current through it. As the semiconductor industry is nearing the limits of performance improvements for the current technologies dominated by silicon, there is a constant search for new, nontraditional materials whose properties can be controlled by the electric field. The most notable recent examples of such materials are organic conductors (*1*) and carbon nanotubes (*2*). It has long been tempting to extend the use of the field effect to metals [e.g., to develop all-metallic transistors that could be scaled down to much smaller sizes and would consume less energy and operate at higher frequencies

[1]Department of Physics, University of Manchester, Manchester M13 9PL, UK. [2]Institute for Microelectronics Technology, 142432 Chernogolovka, Russia.
*To whom correspondence should be addressed. E-mail: geim@man.ac.uk

than tradi
However,
metal fil
screened
and bulk
large com
be induce
tend to b
coming d
eral nanometers; so far, this has proved to be
an insurmountable obstacle to metallic elec-
tr
sl
fi
fi
d
fi
n
d
tu
ti
g
c
graphene sheets rolled up into nanometer-sized
cylinders) (*5–7*). Planar
been presumed not to exi
being unstable with respect
curved structures such as
nanotubes (*5–14*).

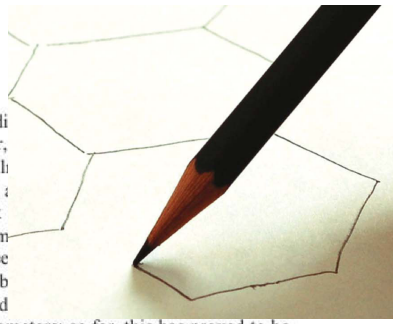

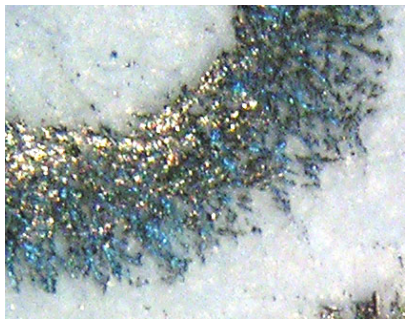

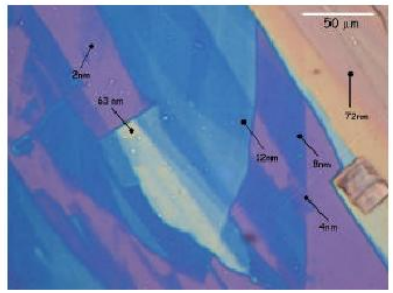

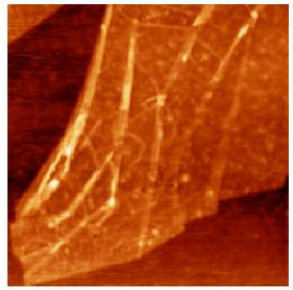

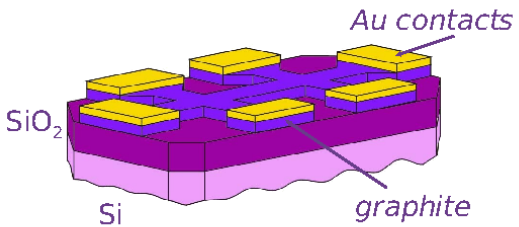

Technology

$$H \approx -t \sum_{i,\tau} \sum_j a_\tau^\dagger(\mathbf{R}_i) b_\tau(\mathbf{R}_i + \delta_j) + c.c.$$

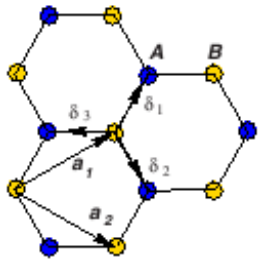

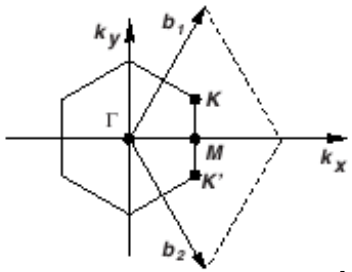

$$a_{\tau;i} = \frac{1}{N} \sum_{\mathbf{k}} e^{-i\mathbf{k}\mathbf{R}_i} a_\tau(\mathbf{k})$$

$$H = -t \sum_{\mathbf{k},\tau} f(\mathbf{k}) a_\tau^\dagger(\mathbf{k}) b_\tau(\mathbf{k}) + c.c.$$

$$H = -t \sum_{\mathbf{k},\tau} \left[a_\tau^\dagger(\mathbf{k}), b_\tau^\dagger(\mathbf{k}) \right] \begin{bmatrix} 0 & f(\mathbf{k}) \\ f^*(\mathbf{k}) & 0 \end{bmatrix} \begin{bmatrix} a_\tau(\mathbf{k}) \\ b_\tau(\mathbf{k}) \end{bmatrix}$$

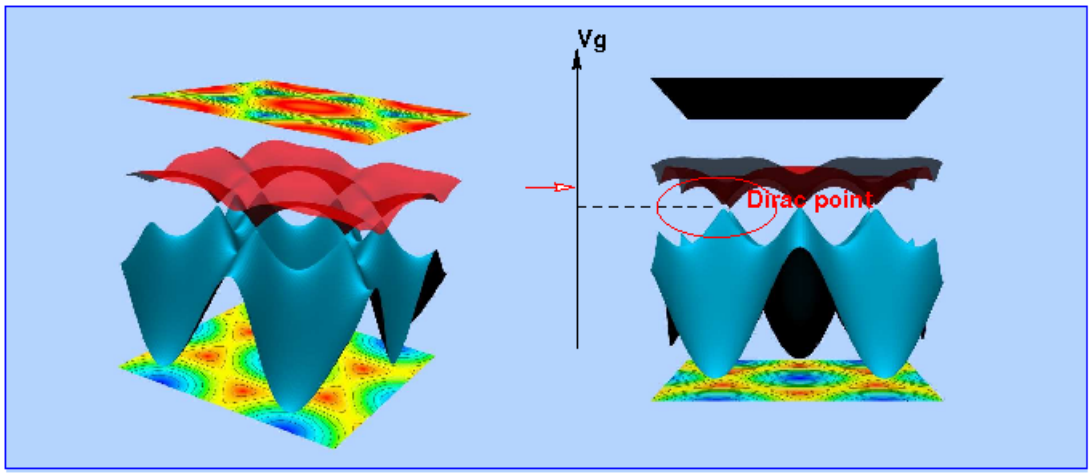

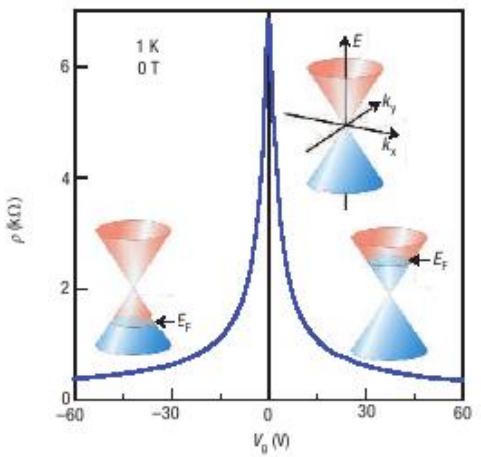

Technology

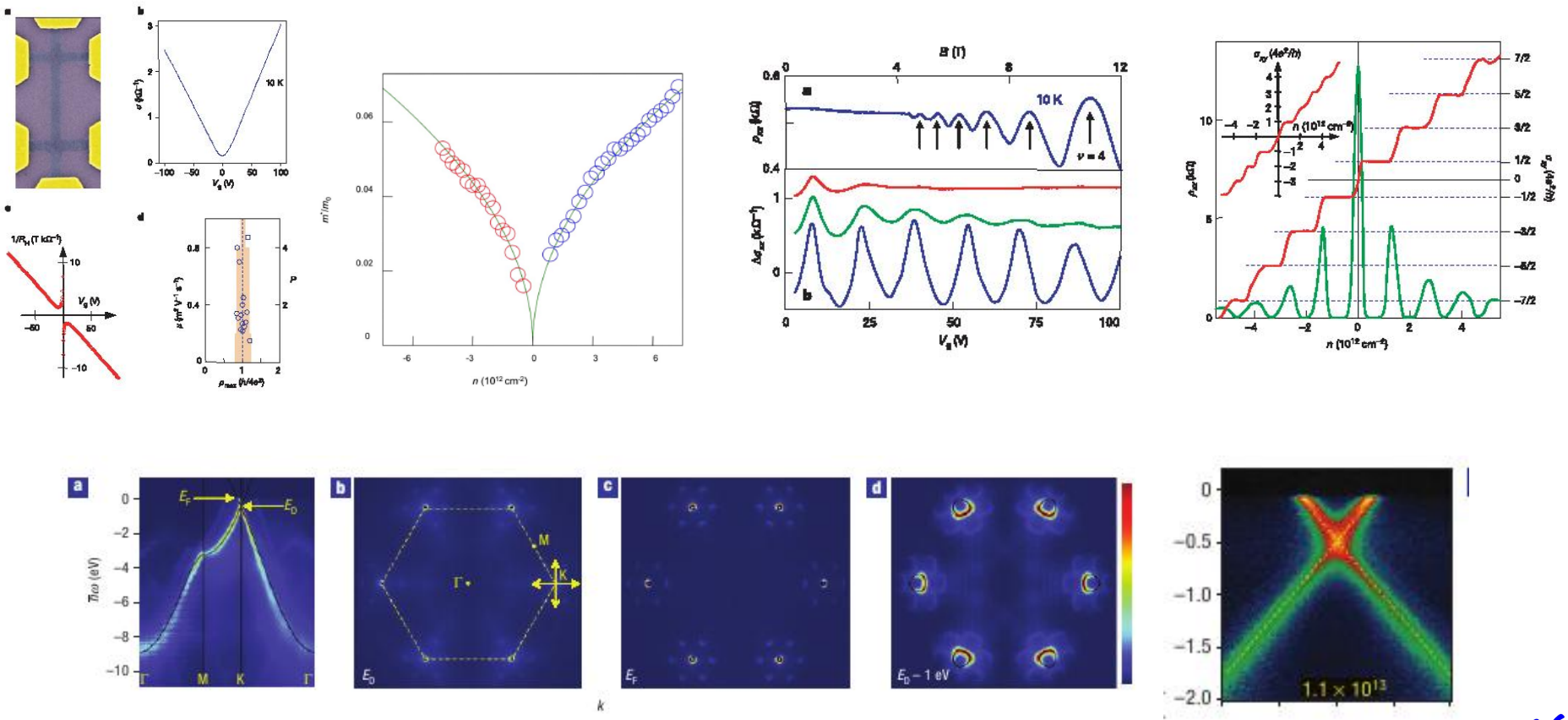

Technology

Graphene is a true 2D-electron gas (2DEG) system with pseudo-relativistic conduction electrons!

...why interesting for us?

- **Chemistry**: graphene is a large polycylic aromatic hydrocarbon
- **Surface Science**: adsorption of atoms/molecules may tremendously affect transport properties

Technology

Graphene is a true 2D-electron gas (2DEG) system with pseudo-relativistic conduction electrons!

...why interesting for us?

- **Chemistry**: graphene is a large polycylic aromatic hydrocarbon
- **Surface Science**: adsorption of atoms/molecules may tremendously affect transport properties

Technology

Graphene is a true 2D-electron gas (2DEG) system with pseudo-relativistic conduction electrons!

...why interesting for us?

- **Chemistry**: graphene is a large polycylic aromatic hydrocarbon
- **Surface Science**: adsorption of atoms/molecules may tremendously affect transport properties

The need for understanding adsorption

H on Graphite (Graphene) *vs* metal substrates

- Chemisorption is thermally activated[1,2]
- Substantial lattice reconstruction upon sticking[1,2]
- Diffusion of chemisorbed H atoms does not occur[3]
- Preferential sticking[3]
- Clustering of H atoms[3,4,5]
- Dimer recombination[6]

[1] L. Jeloaica and V. Sidis, *Chem. Phys. Lett.* 300, 157 (1999) [2] X. Sha and B. Jackson, *Surf. Sci.* 496, 318 (2002)

[3] L. Hornekaer *et al.*, *Phys. Rev. Lett.* 97, 186102 (2006) [4] A. Andree *et al.*, *Chem. Phys. Lett.* 425, 99 (2006) [5]

L. Hornekaer *et al.*, *Chem. Phys. Lett.* 446, 237 (2007) [6] L. Hornekaer *et al.*, *Phys. Rev. Lett.* 96, 156104 (2006)

Theoretical tools

I. Tight-binding π Hamiltonian (uncorrelated e^-)

$$H \approx H^{TB} = \sum_{\tau,ij}(t_{ij}a^{\dagger}_{i,\tau}b_{j,\tau} + t_{ji}b^{\dagger}_{j,\tau}a_{i,\tau}) + next - to - nn + etc...$$

II. Hubbard (partially correlated e^-)

$$H \approx H^{TB} + \sum_i U_i n_{i,\uparrow} n_{i,\downarrow}$$

$\Longleftrightarrow$

III. Valence-Bond (partially correlated e^-)

$$\Psi_{VB} = \mathcal{A}\{\phi_1\phi_2\phi_3...\phi_N\Theta^N_{S,M}\}$$

IV. DFT calculations ('fully' correlated e^-) and more..

- Periodic, plane-wave based, spin-polarized calculations with VASP
- PAW method, PBE functional
- 5x5x1 unit cell, c=20 Å (vacuum), 6x6x1 Γ-centered k mesh, E_{cut} = 500 eV

Theoretical tools

I. Tight-binding π Hamiltonian (uncorrelated e^-)

$$H \approx H^{TB} = \sum_{\tau,ij}(t_{ij}a^{\dagger}_{i,\tau}b_{j,\tau} + t_{ji}b^{\dagger}_{j,\tau}a_{i,\tau}) + next - to - nn + etc...$$

II. Hubbard (partially correlated e^-)

$$H \approx H^{TB} + \sum_i U_i n_{i,\uparrow} n_{i,\downarrow}$$

$\Longleftrightarrow$

III. Valence-Bond (partially correlated e^-)

$$\Psi_{VB} = \mathcal{A}\{\phi_1\phi_2\phi_3...\phi_N\Theta^N_{S,M}\}$$

IV. DFT calculations ('fully' correlated e^-) and more..

- Periodic, plane-wave based, spin-polarized calculations with VASP
- PAW method, PBE functional
- 5x5x1 unit cell, c=20 Å (vacuum), 6x6x1 Γ-centered k mesh, E_{cut} = 500 eV

Theoretical tools

I. Tight-binding π Hamiltonian (uncorrelated e^-)

$$H \approx H^{TB} = \sum_{\tau,ij}(t_{ij}a^{\dagger}_{i,\tau}b_{j,\tau} + t_{ji}b^{\dagger}_{j,\tau}a_{i,\tau}) + next - to - nn + etc...$$

II. Hubbard (partially correlated e^-)

$$H \approx H^{TB} + \sum_i U_i n_{i,\uparrow} n_{i,\downarrow}$$

$\Longleftrightarrow$

III. Valence-Bond (partially correlated e^-)

$$\Psi_{VB} = \mathcal{A}\{\phi_1\phi_2\phi_3...\phi_N\Theta^N_{S,M}\}$$

IV. DFT calculations ('fully' correlated e^-) and more..

- Periodic, plane-wave based, spin-polarized calculations with VASP
- PAW method, PBE functional
- 5x5x1 unit cell, c=20 Å (vacuum), 6x6x1 Γ-centered k mesh, E_{cut} = 500 eV

Theoretical tools

I. Tight-binding π Hamiltonian (uncorrelated e^-)

$$H \approx H^{TB} = \sum_{\tau,ij}(t_{ij}a^{\dagger}_{i,\tau}b_{j,\tau} + t_{ji}b^{\dagger}_{j,\tau}a_{i,\tau}) + next - to - nn + etc...$$

II. Hubbard (partially correlated e^-)

$$H \approx H^{TB} + \sum_i U_i n_{i,\uparrow} n_{i,\downarrow}$$

$\Longleftrightarrow$

III. Valence-Bond (partially correlated e^-)

$$\Psi_{VB} = \mathcal{A}\{\phi_1\phi_2\phi_3...\phi_N\Theta^N_{S,M}\}$$

IV. DFT calculations ('fully' correlated e^-) and more..

- Periodic, plane-wave based, spin-polarized calculations with VASP
- PAW method, PBE functional
- 5x5x1 unit cell, c=20 Å (vacuum), 6x6x1 Γ-centered k mesh, E_{cut} = 500 eV

Theoretical tools

I. Tight-binding π Hamiltonian (uncorrelated e^-)

$$H \approx H^{TB} = \sum_{\tau,ij}(t_{ij}a^{\dagger}_{i,\tau}b_{j,\tau} + t_{ji}b^{\dagger}_{j,\tau}a_{i,\tau}) + next - to - nn + etc...$$

II. Hubbard (partially correlated e^-)

$$H \approx H^{TB} + \sum_i U_i n_{i,\uparrow} n_{i,\downarrow}$$

$\Longleftrightarrow$

III. Valence-Bond (partially correlated e^-)

$$\Psi_{VB} = \mathcal{A}\{\phi_1\phi_2\phi_3...\phi_N\Theta^N_{S,M}\}$$

IV. DFT calculations ('fully' correlated e^-) and more..

- Periodic, plane-wave based, spin-polarized calculations with VASP
- PAW method, PBE functional
- 5x5x1 unit cell, c=20 Å (vacuum), 6x6x1 Γ-centered k mesh, E_{cut} = 500 eV

I. Properties of *bipartite* lattices

$$H^{TB} = \sum_{\sigma,ij}(t_{ij}a^{\dagger}_{i,\sigma}b_{j,\sigma} + t_{ji}b^{\dagger}_{j,\sigma}a_{i,\sigma})$$

Electron-hole symmetry

$$b_i \longrightarrow -b_i \Longrightarrow \mathbf{h} \longrightarrow -\mathbf{h}$$

if ϵ_i is eigenvalue and
$c_i^{\dagger} = \sum_i \alpha_i a_i^{\dagger} + \sum_j \beta_j b_j^{\dagger}$ eigenvector

$\Downarrow$

$-\epsilon_i$ is also eigenvalue and
$c_i'^{\dagger} = \sum_i \alpha_i a_i^{\dagger} - \sum_j \beta_j b_j^{\dagger}$ is eigenvector

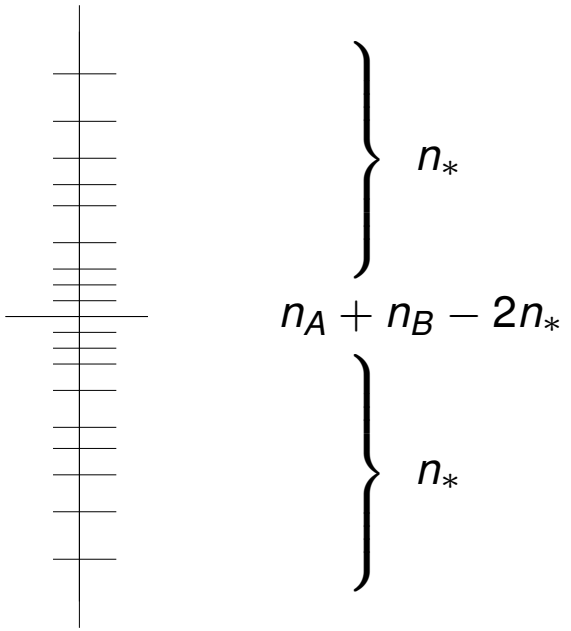

I. Properties of *bipartite* lattices

$$H^{TB} = \sum_{\tau,ij}(t_{ij}a^{\dagger}_{i,\tau}b_{j,\tau} + t_{ji}b^{\dagger}_{j,\tau}a_{i,\tau})$$

Theorem

If $n_A > n_B$ there exist (at least) $n_l = n_A - n_B$ "midgap states" with vanishing components on B sites

Proof.

$$\begin{bmatrix} \mathbf{0} & \mathbf{T}^{\dagger} \\ \mathbf{T} & \mathbf{0} \end{bmatrix} \begin{bmatrix} \boldsymbol{\alpha} \\ \boldsymbol{\beta} \end{bmatrix} = \begin{bmatrix} \mathbf{0} \\ \mathbf{0} \end{bmatrix} \text{ with } \mathbf{T}\ n_B x n_A(\ > n_B)$$

$$\Longrightarrow \mathbf{T}\boldsymbol{\alpha} = \mathbf{0} \text{ has } n_A - n_B \text{ solutions}$$

□

II. Properties of *bipartite* lattices

$$H^{Hb} = \sum_{\tau,ij}(t_{ij}a^{\dagger}_{i,\tau}b_{j,\tau} + t_{ji}b^{\dagger}_{j,\tau}a_{i,\tau}) + U\sum_i n_{i,\tau}n_{i,-\tau}$$

Theorem

If $U > 0$, the ground-state at half-filling has

$$S = |n_A - n_B|/2 = n_I/2$$

Proof.

E.H. Lieb, *Phys. Rev. Lett.* **62** (1989) 1201 □

...basically, we can apply Hund's rule to previous result

Bipartite lattices: theorems at work

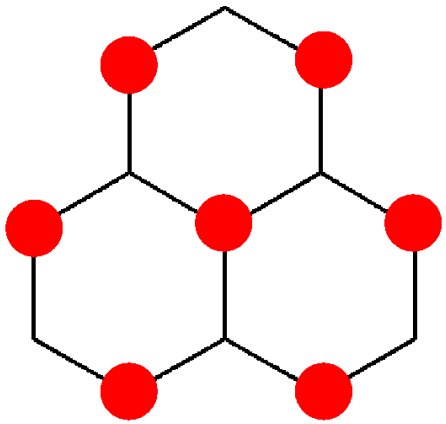

$n_A = n_B + 1$
$S = 1/2$

patterned spin-density..

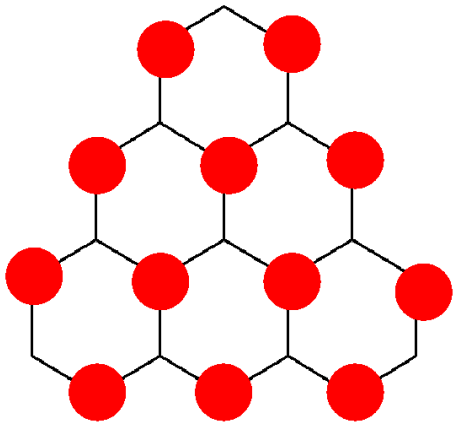

$n_A = n_B + 2$
$S = 1$

..triplet ground-state

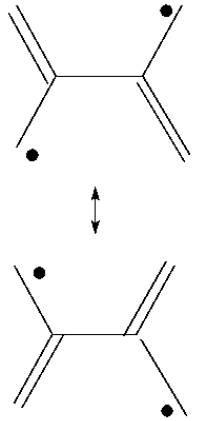

$n_A = n_B$
$S = 0$

'open-shell singlet'

Bipartite lattices: theorems at work

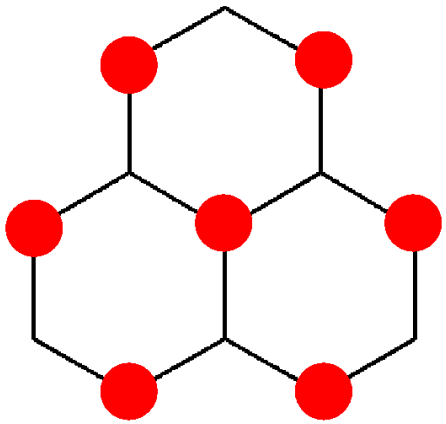

$n_A = n_B + 1$

$S = 1/2$

patterned spin-density..

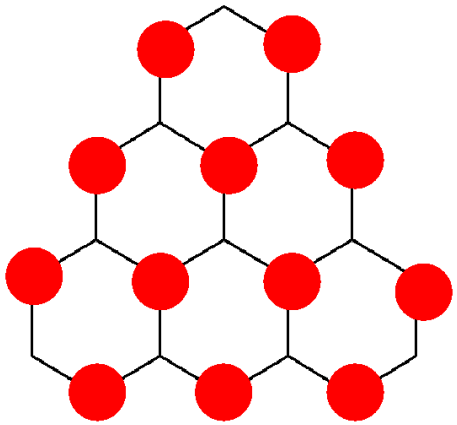

$n_A = n_B + 2$

$S = 1$

..triplet ground-state

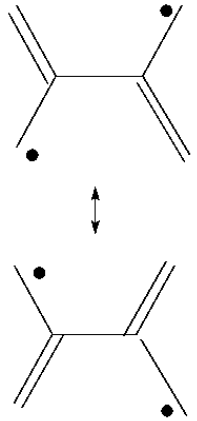

$n_A = n_B$

$S = 0$

‘open-shell singlet’

Bipartite lattices: theorems at work

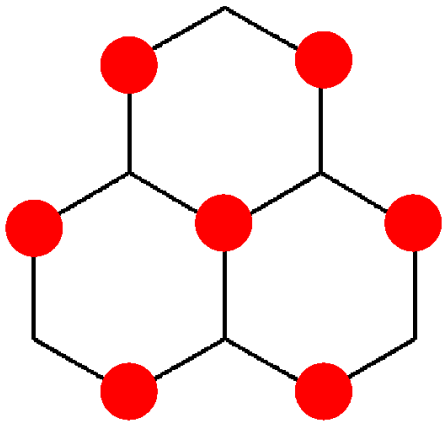

$n_A = n_B + 1$

$S = 1/2$

patterned spin-density..

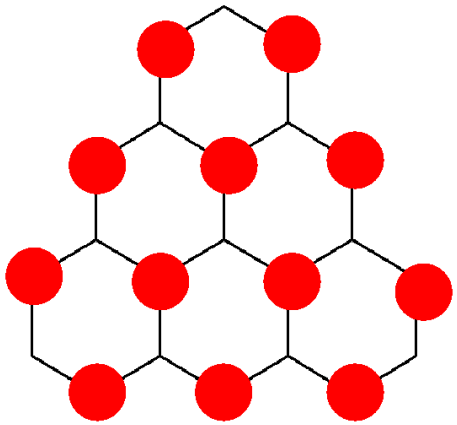

$n_A = n_B + 2$

$S = 1$

..triplet ground-state

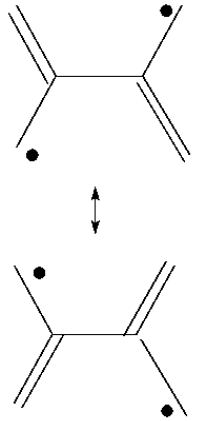

$n_A = n_B$

$S = 0$

'open-shell singlet'

Bipartite lattices: theorems at work

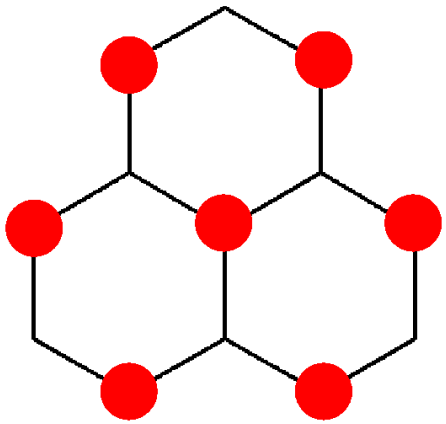

$n_A = n_B + 1$

$S = 1/2$

patterned spin-density..

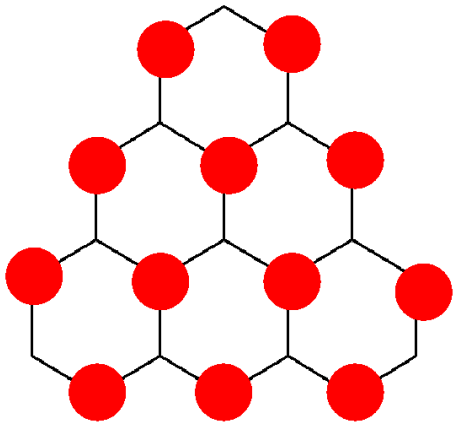

$n_A = n_B + 2$

$S = 1$

..triplet ground-state

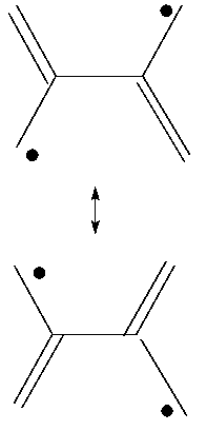

$n_A = n_B$

$S = 0$

'open-shell singlet'

III. Valence Bond picture

Modern, basic VB *ansatz*

$$\Psi = \mathcal{A}\{\phi_1\phi_2\phi_3\ldots\phi_N\Theta^N_{S,M}\}$$

$$\Theta^N_{S,M} = \sum_k^{f_s^N} c_k\Theta^N_{S,M;k}$$

- orbitals ϕ_i are (or turn out to be) localized on atoms
- spin-function is the best coupling for the given S

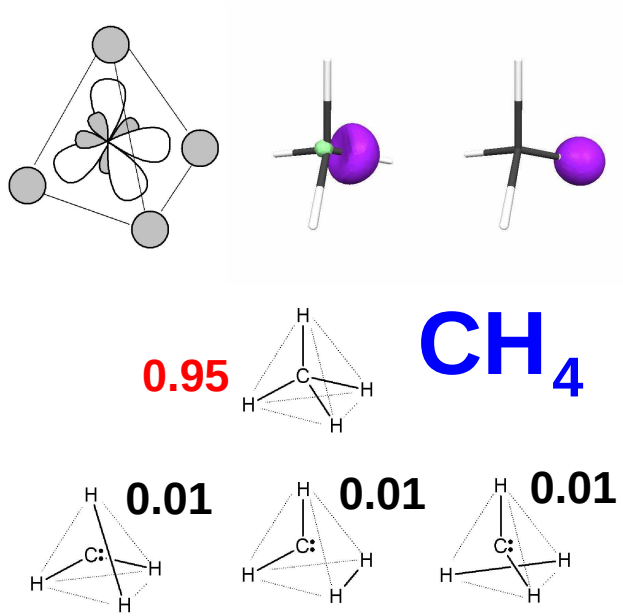

$$\Psi = \sum_{k=1}^{42} c_k\mathcal{A}\{\phi_1..\phi_{10}\Theta^{10}_{0,0;k}\}$$
$$\sim \mathcal{A}\{\phi_1..\phi_{10}\Theta^{PP}\}$$

III. Valence Bond picture

Modern, basic VB *ansatz*

$$\Psi = \mathcal{A}\{\phi_1\phi_2\phi_3\ldots\phi_N\Theta^N_{S,M}\}$$

$$\Theta^N_{S,M} = \sum_k^{f_s^N} c_k\Theta^N_{S,M;k}$$

- orbitals ϕ_i are (or turn out to be) localized on atoms
- spin-function is the best coupling for the given S

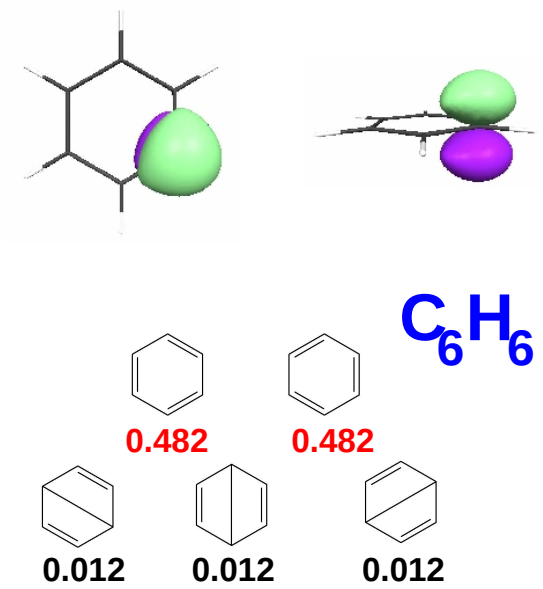

$$\Psi = \sum_{k=1}^{6} c_k\mathcal{A}\{\phi_1\phi_2\phi_3\phi_4\phi_5\phi_6\Theta^6_{0,0;k}\}$$

III. Valence Bond picture

Modern, basic VB *ansatz*

$$\Psi = \mathcal{A}\{\phi_1\phi_2\phi_3...\phi_N\Theta^N_{S,M}\}$$

$$\Theta^N_{S,M} = \sum_k^{f_s^N} c_k \Theta^N_{S,M;k}$$

- orbitals ϕ_i are (or turn out to be) localized on atoms
- spin-function is the best coupling for the given S

Kekule (1865)

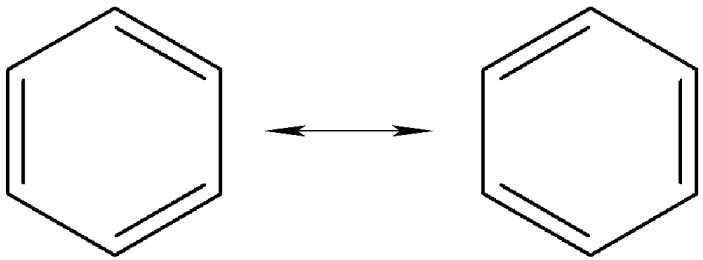

$$\Psi \simeq \Psi_1^{kek} + \Psi_2^{kek}$$

Outline

Adsorption PES

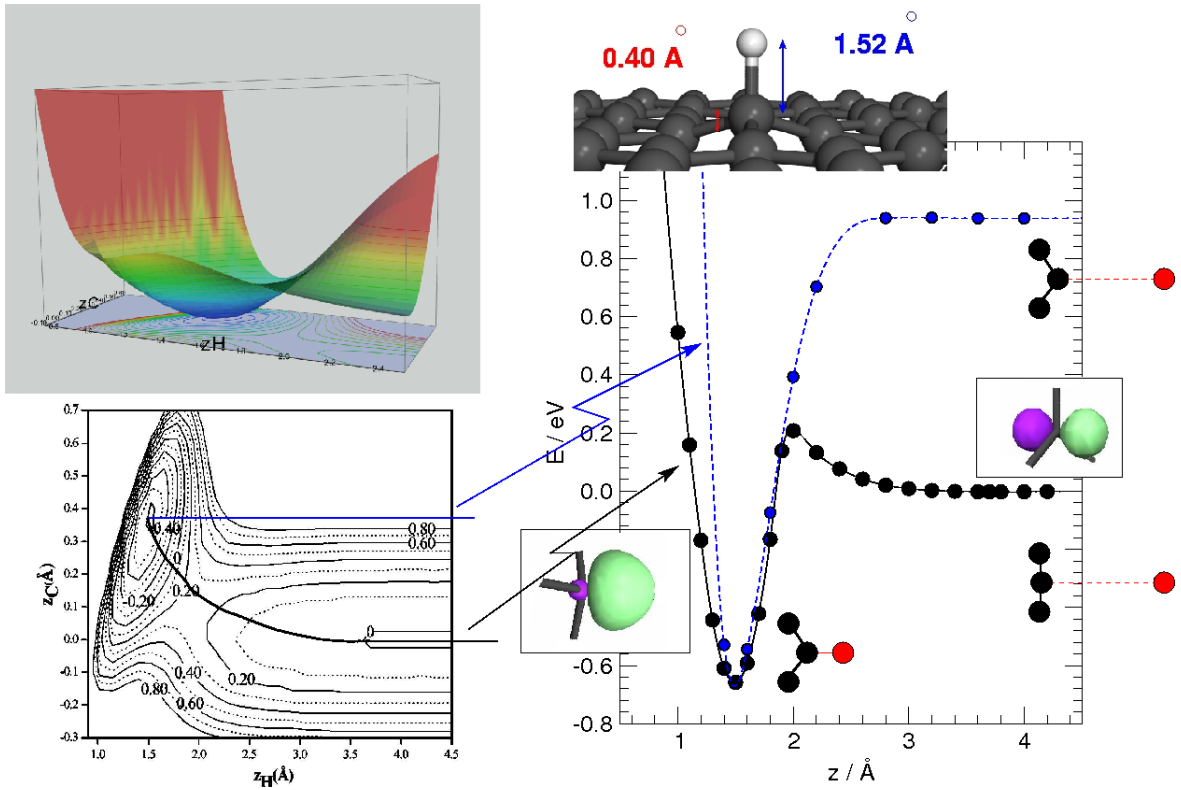

X. Sha and B. Jackson, *Surf. Sci.* 496, 318 (2002)

Valence Bond: adsorption barrier

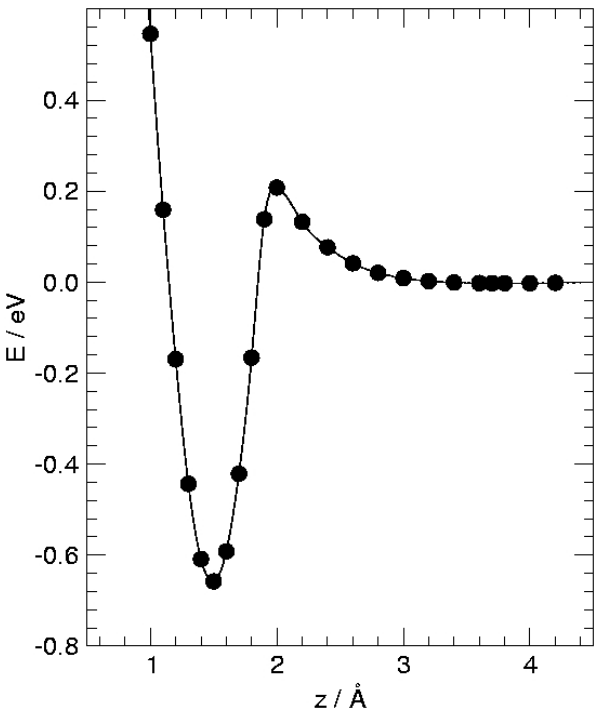

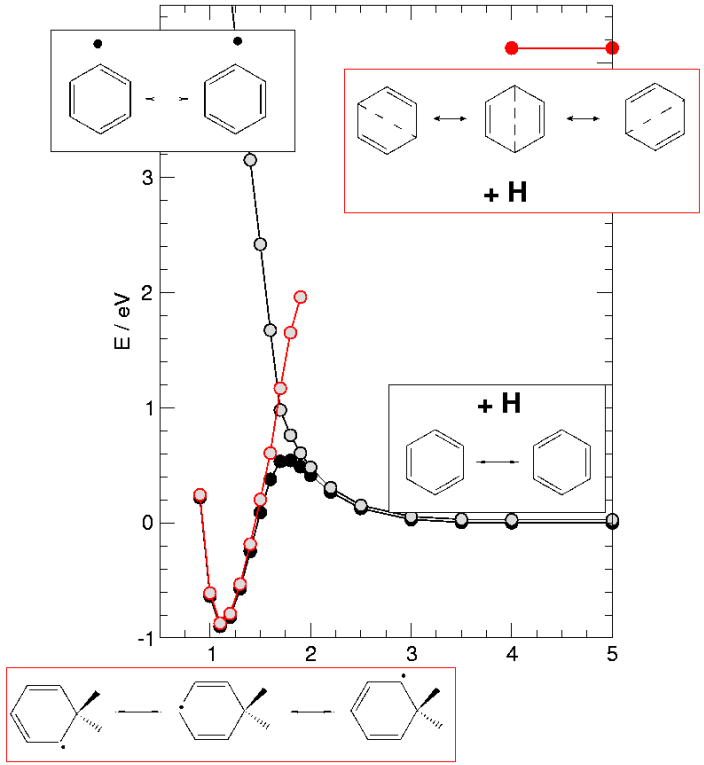

Substrate electronic structure

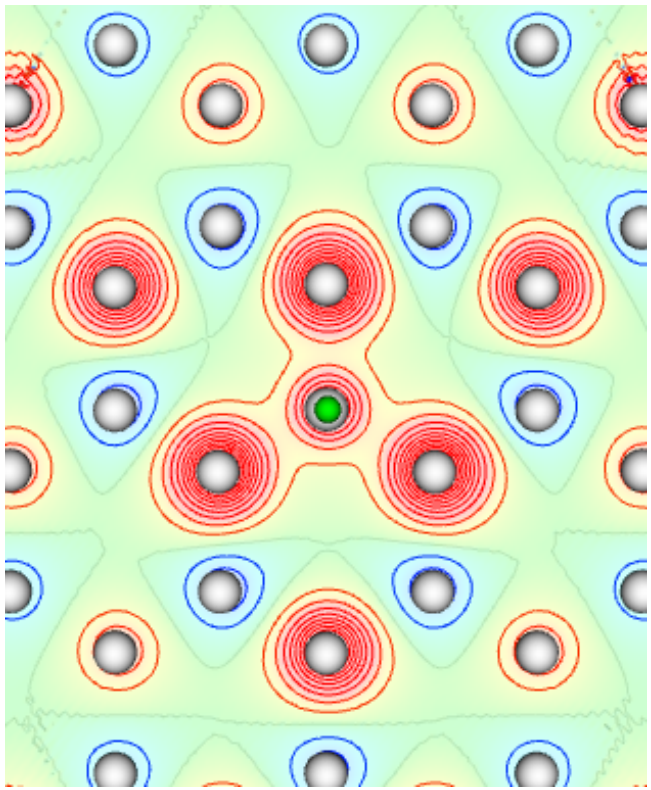

..*patterned* spin-density

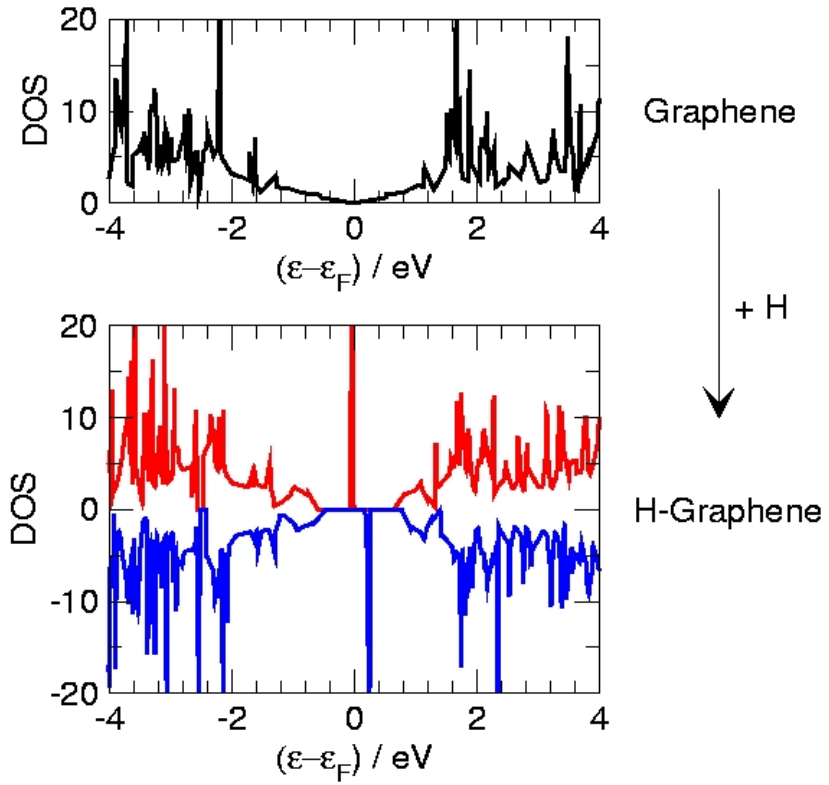

Substrate electronic structure

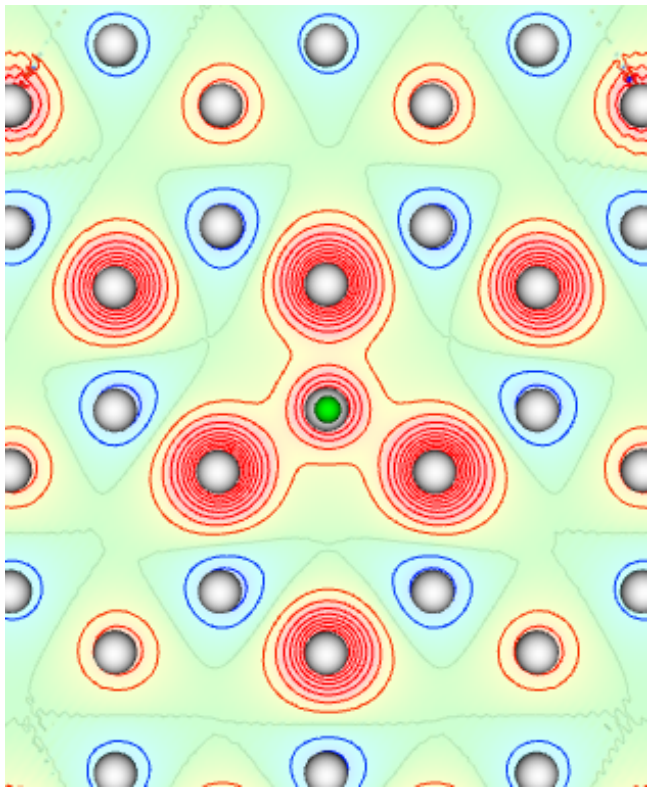

..*patterned* spin-density

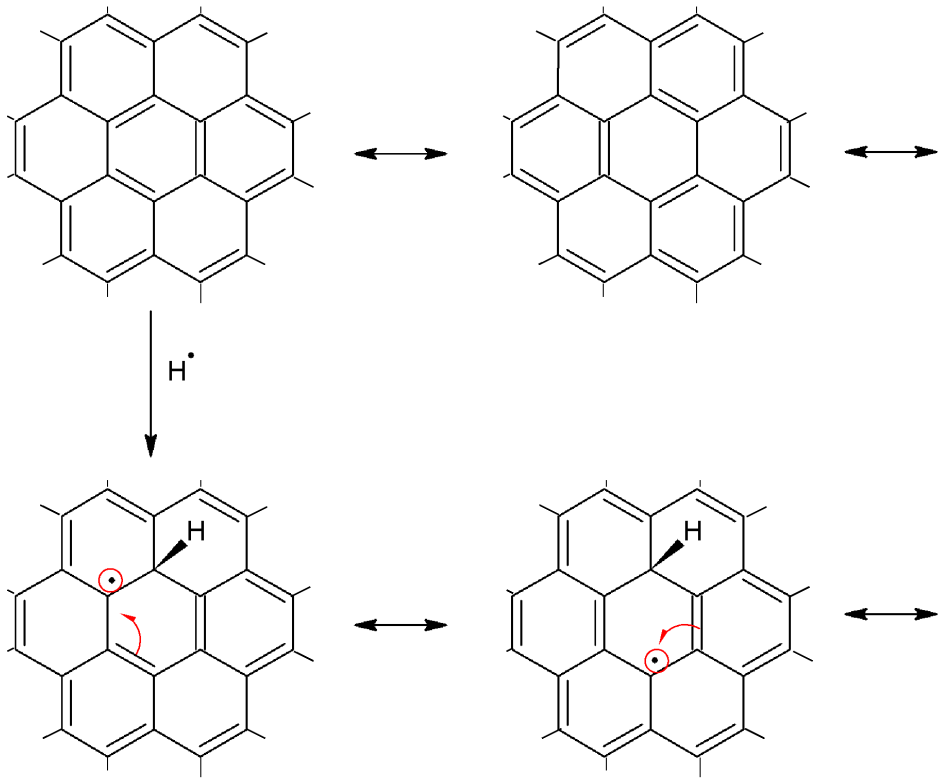

Dimers

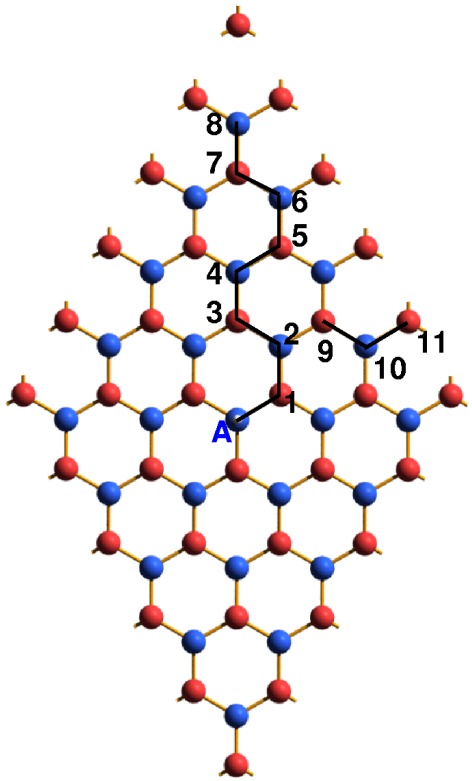
8
7
6
5
4
3
2
9
11
10
1
A

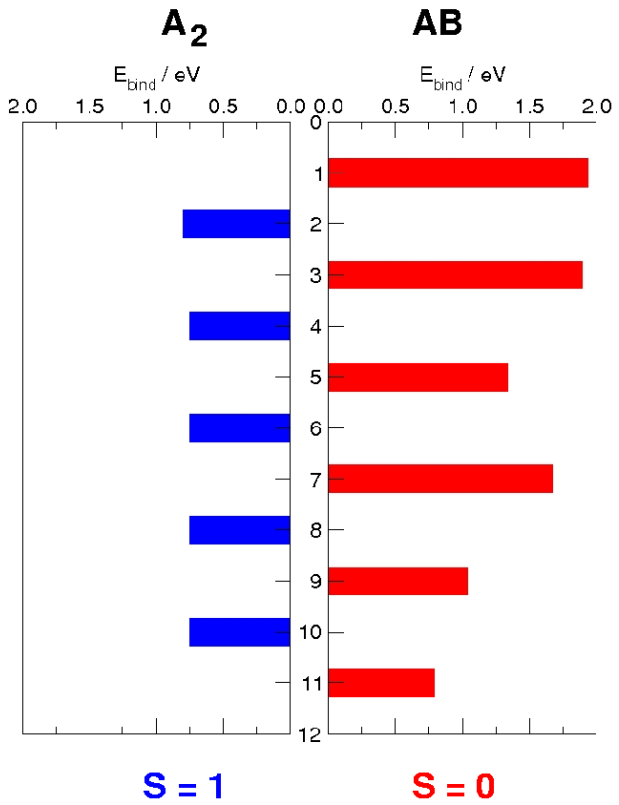
A2
AB
Ebind / eV
Ebind / eV
2.0 1.5 1.0 0.5 0.0
0.0 0.5 1.0 1.5 2.0
0 1 2 3 4 5 6 7 8 9 10 11 12
S = 1
S = 0

Dimers

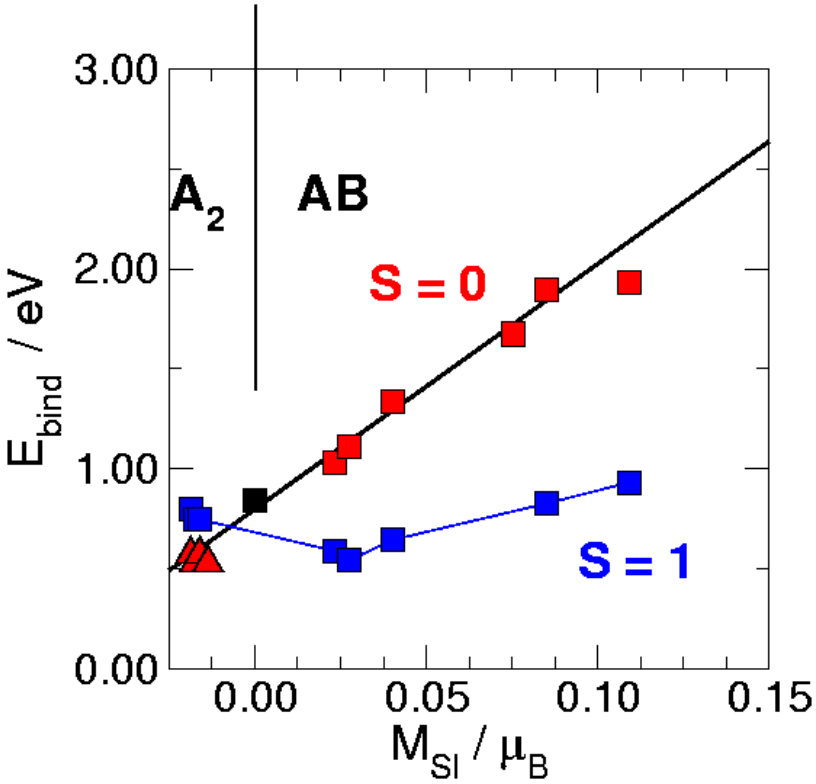

Binding energies depend $\sim$ linearly on the site integrated magnetization (M_{Sl})

Dimers

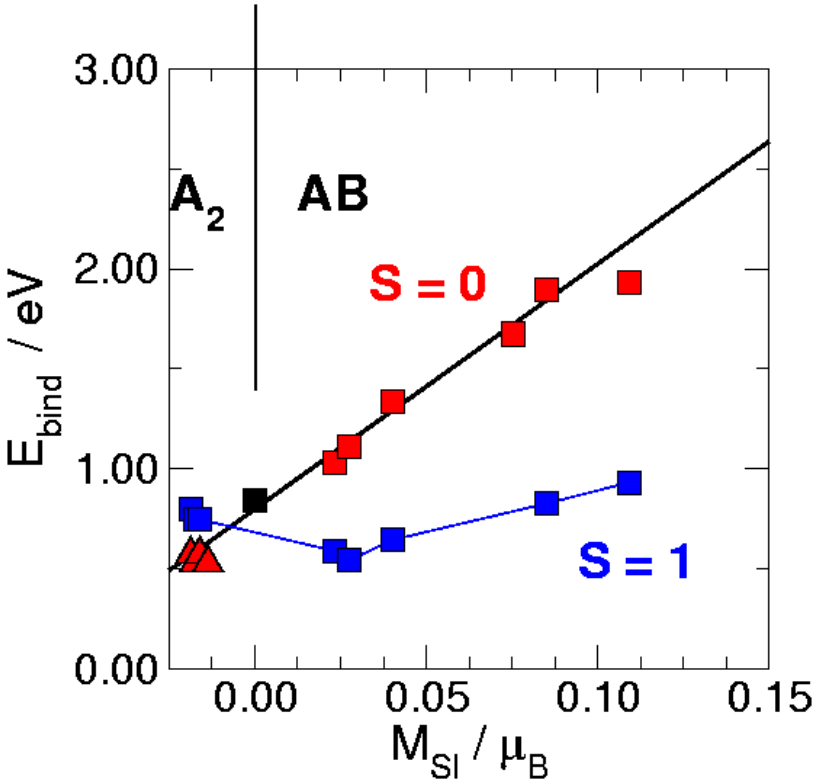
3.00
2.00
1.00
0.00
E_{bind} / eV
A_2
AB
S = 0
S = 1
0.00
0.05
0.10
0.15
M_{SI} / μ_B

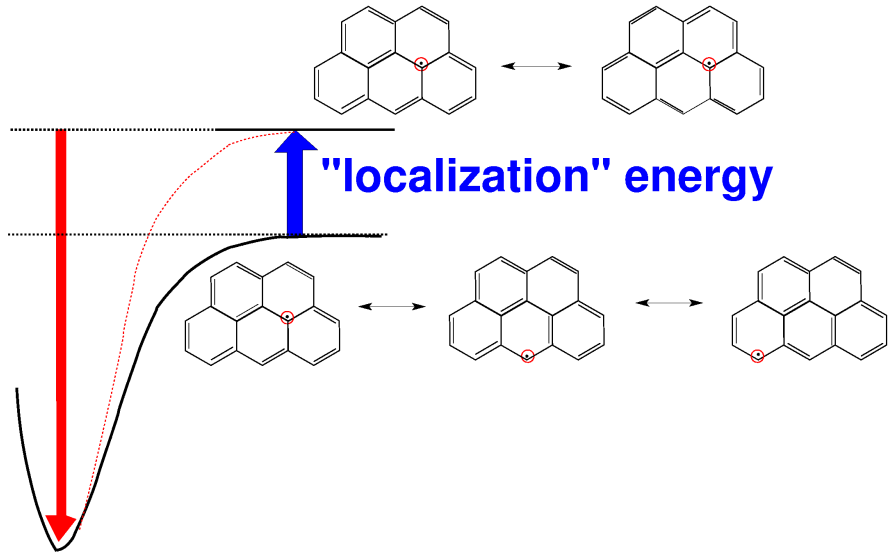
"localization" energy

Dimers

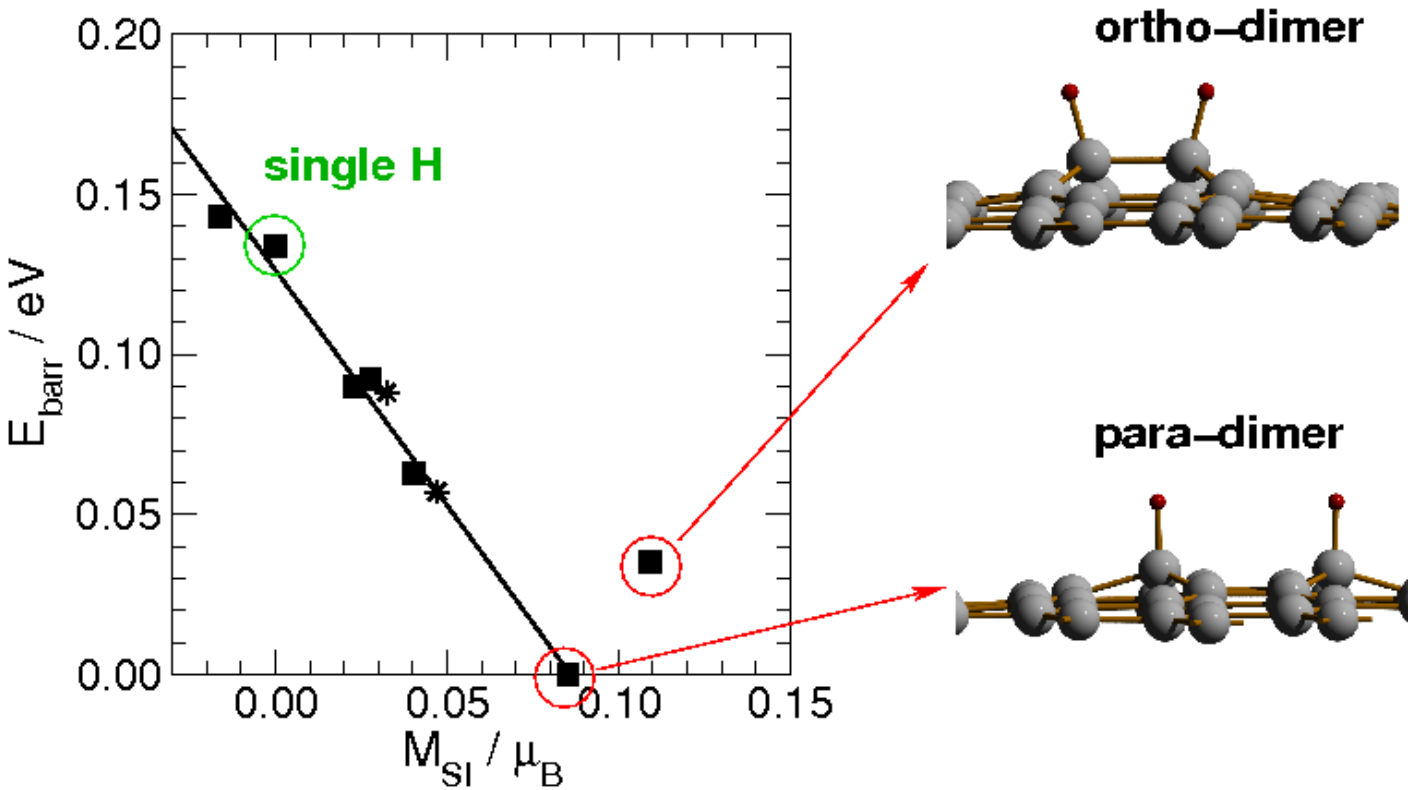
0.20
0.15
0.10
0.05
0.00
E_barr / eV
single H
0.00
0.05
0.10
0.15
M_SI / μ_B
ortho–dimer
para–dimer

Dimers

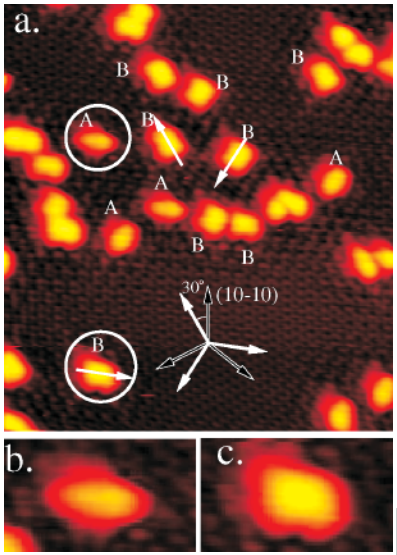

[1]

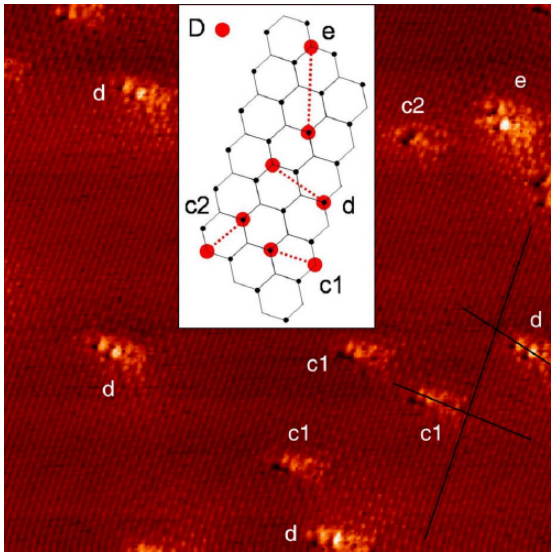

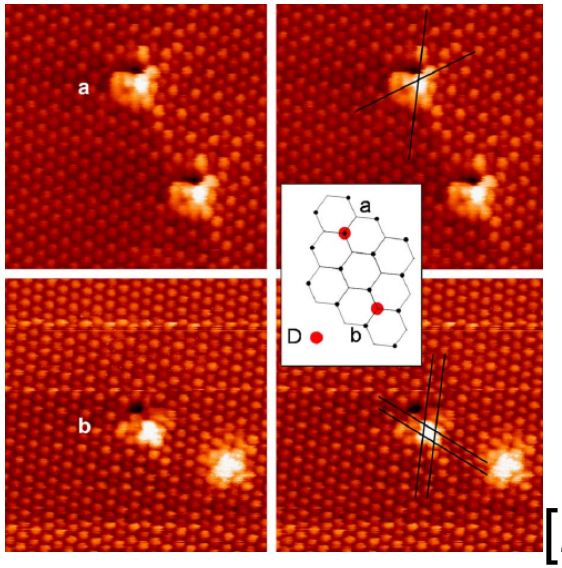

[2]

[1] L. Hornekaer, Z. Sljivancanin, W. Xu, R. Otero, E. Rauls, I. Stensgaard, E. Laegsgaard, B. Hammer and F. Besenbacher. Phys. Rev. Lett. 96 156104 (2006)

[2] A. Andree, M. Le Lay, T. Zecho and J. Kupper, Chem. Phys. Lett. 425 99 (2006)

3-atom clusters

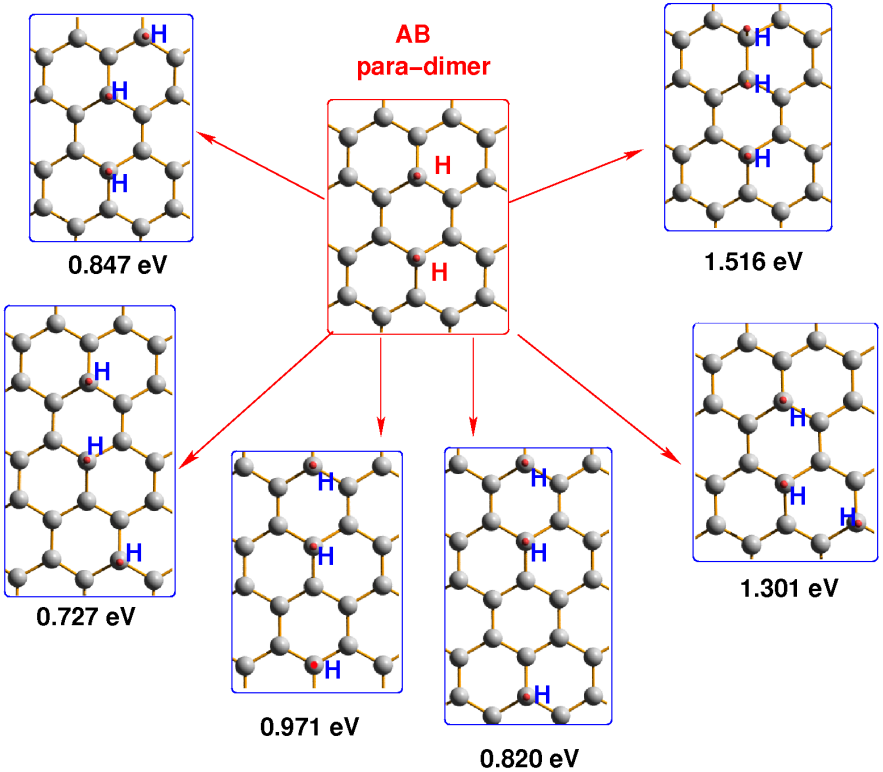

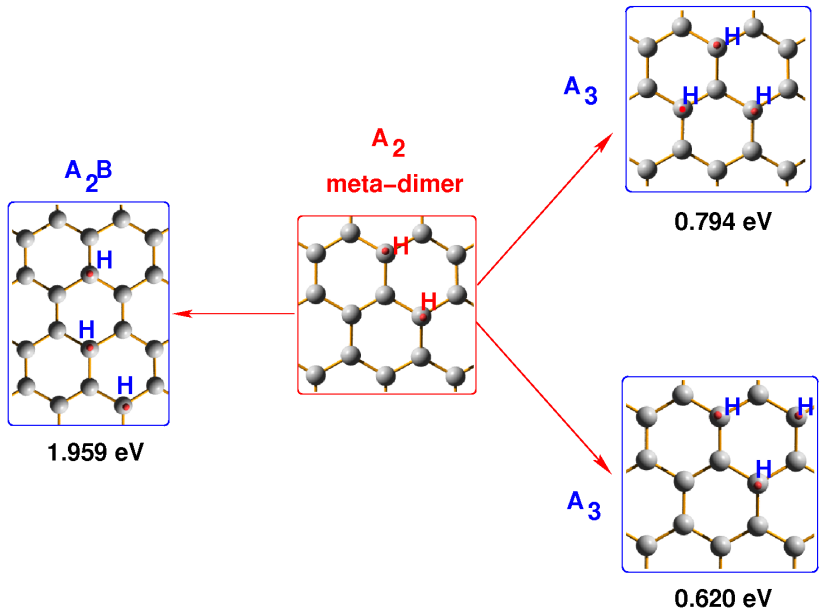

$$\mu = 1\mu_B \Rightarrow \mu = 2\mu_B \Rightarrow \mu = 3\mu_B$$

3-atom clusters

A_2B

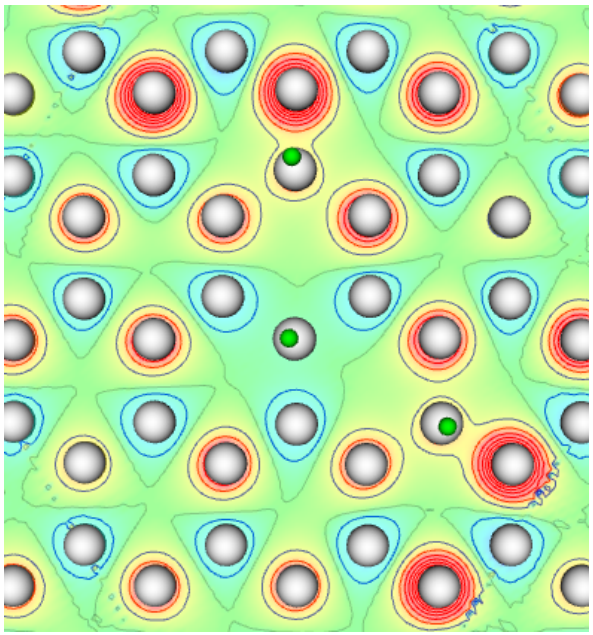

A_3

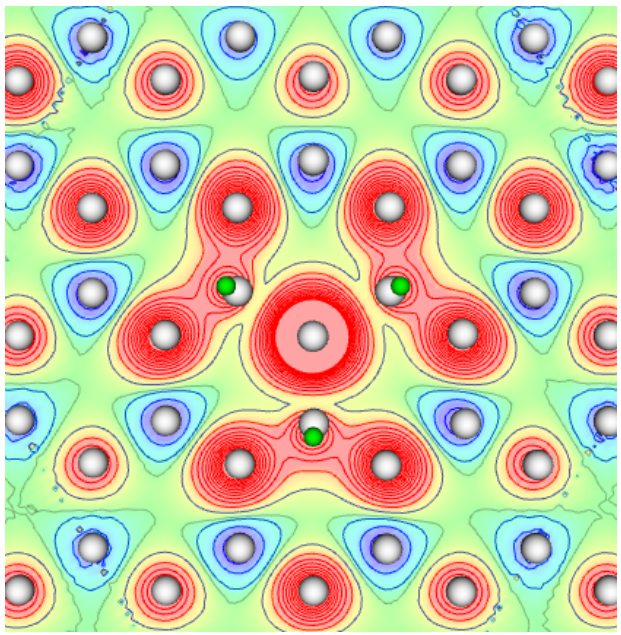

4-atom clusters

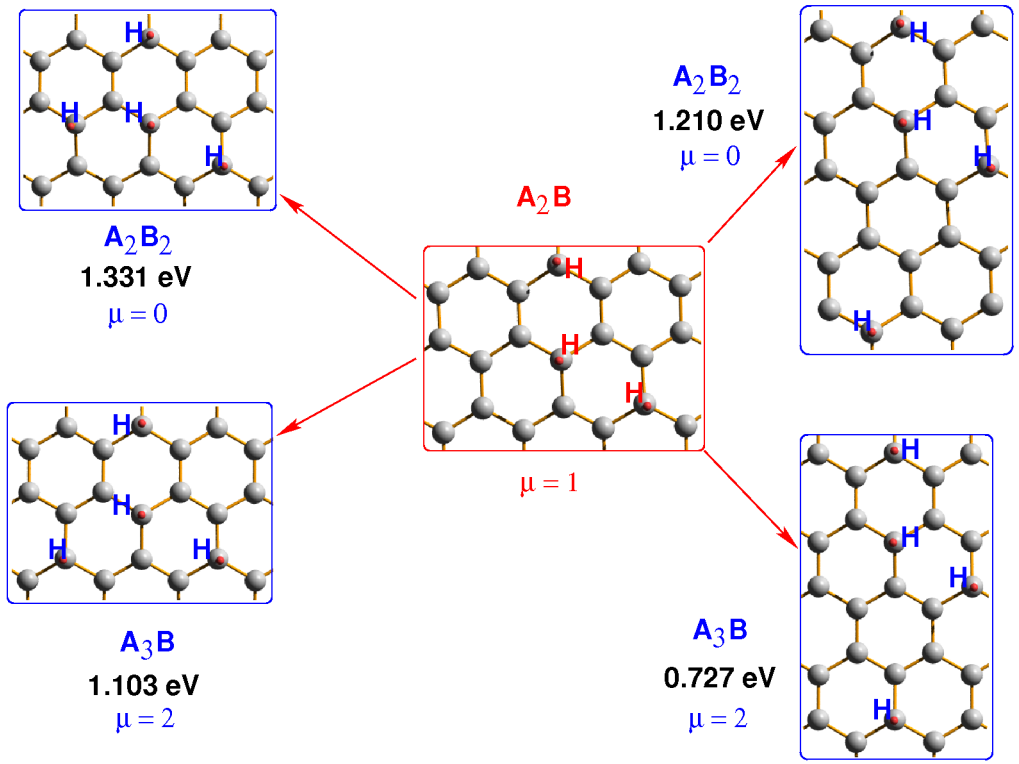

Role of edges

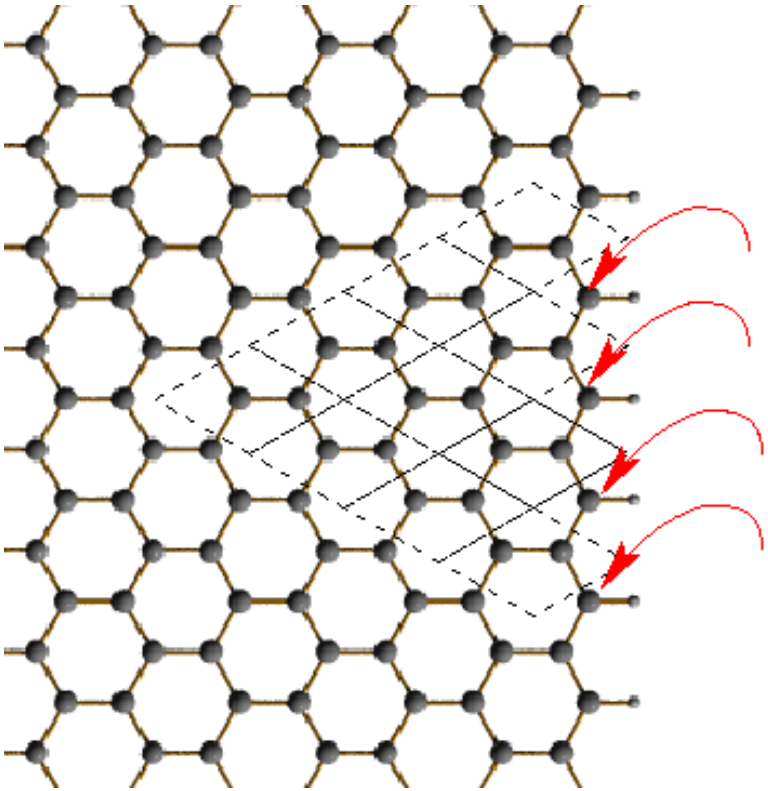

- *zig-zag* edges have enhanced hydrogen affinity
- geometric effects can be investigated in small graphenes

$\Rightarrow$ DFT and Multi-Reference Quasi-Degenerate PT on CASSCF wavefunctions

Systems

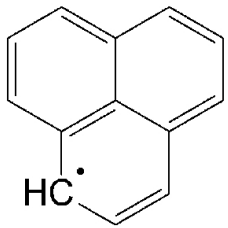

perinaftenile / fenalene

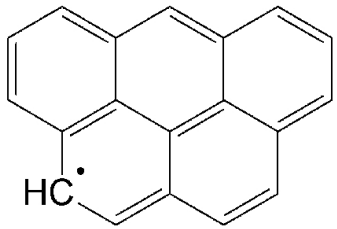

benzo[cd]pirenile

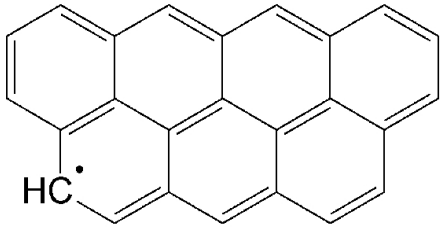

7 - PAH

imbalanced ‘PAHs’

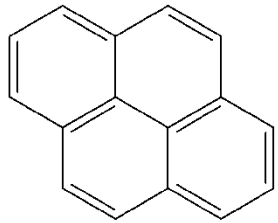

pirene

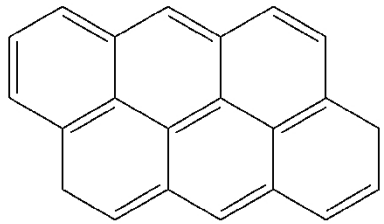

dibenzo[def,mno]crisene / antrantrene

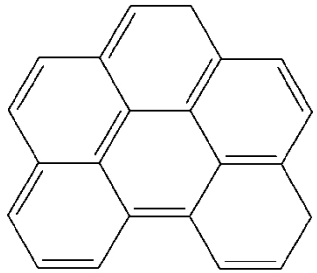

benzo[ghi]perilene

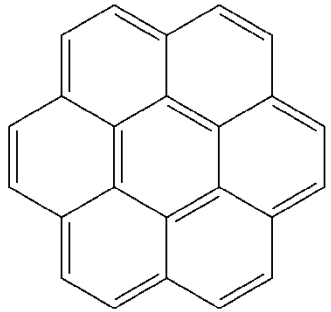

coronene

balanced PAHs

Systems

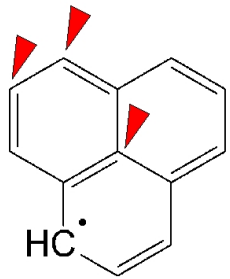

perinaftenile / fenalene

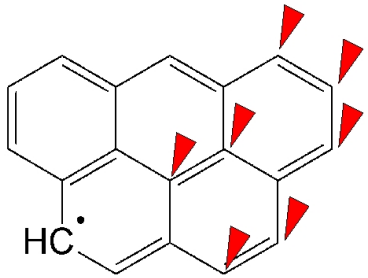

benzo[cd]pirenile

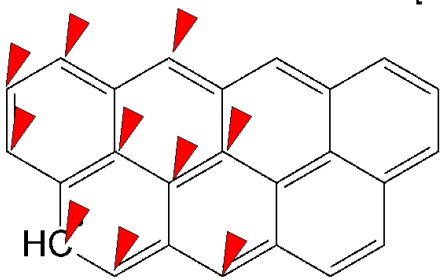

7 - PAH

imbalanced ‘PAHs’

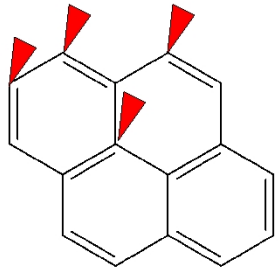

pirene

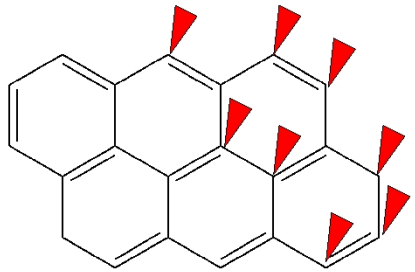

dibenzo[def,mno]crisene / antrantrene

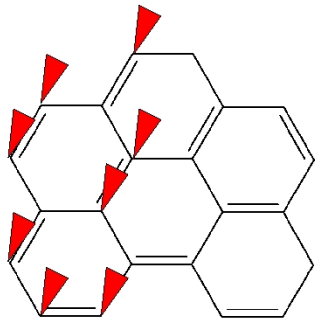

benzo[ghi]perilene

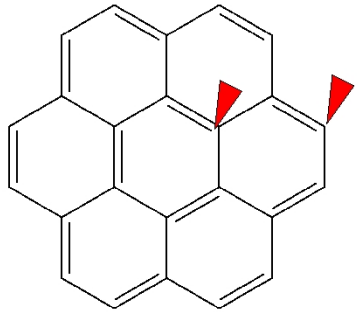

coronene

balanced PAHs

Balanced PAHs

Graphitic *vs* edge carbons

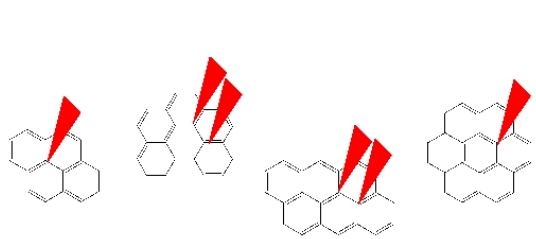

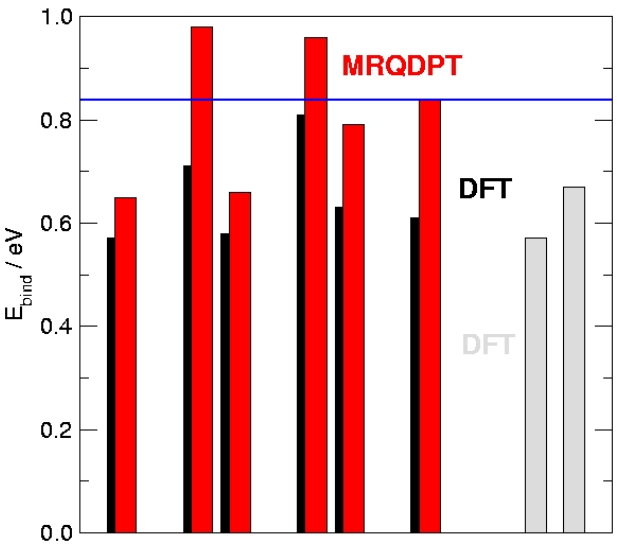

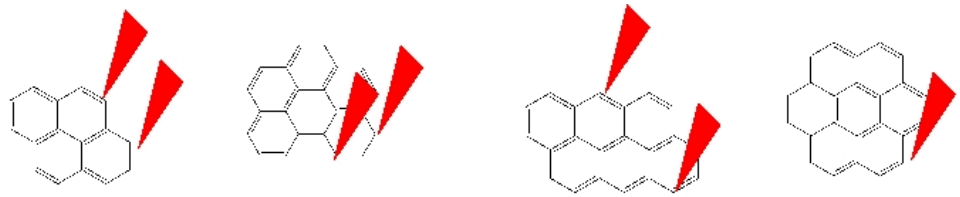

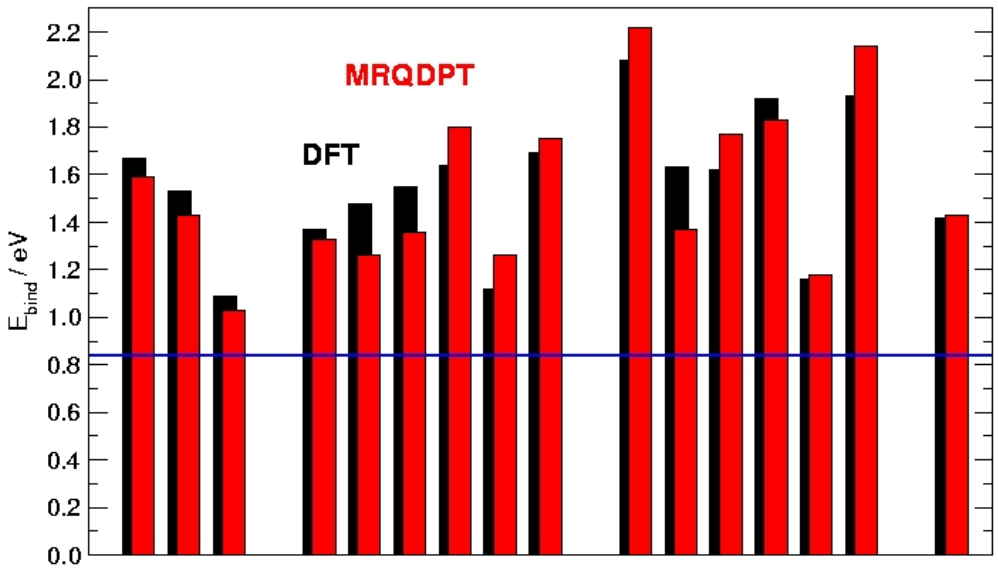

Adsorption paths

Balanced PAH

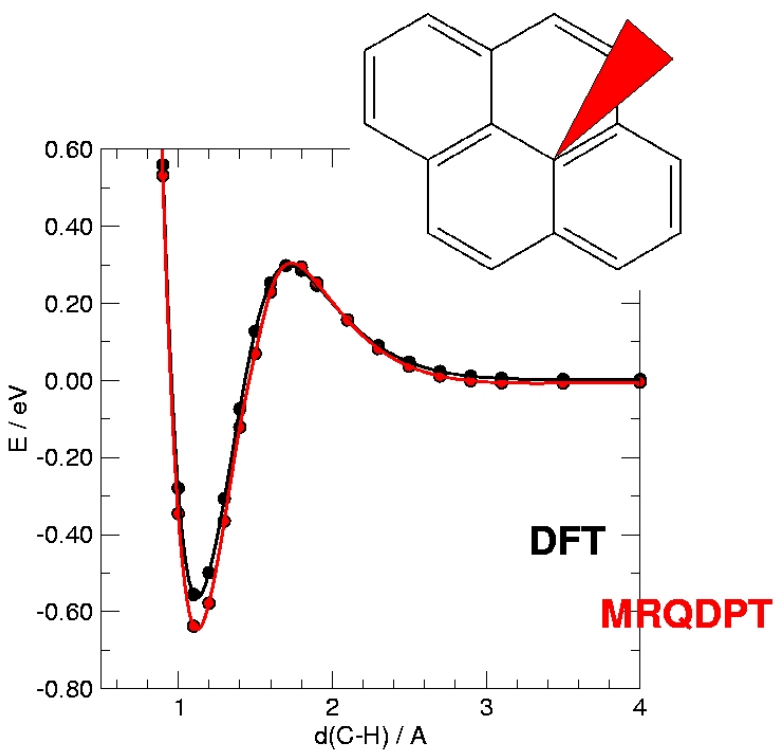

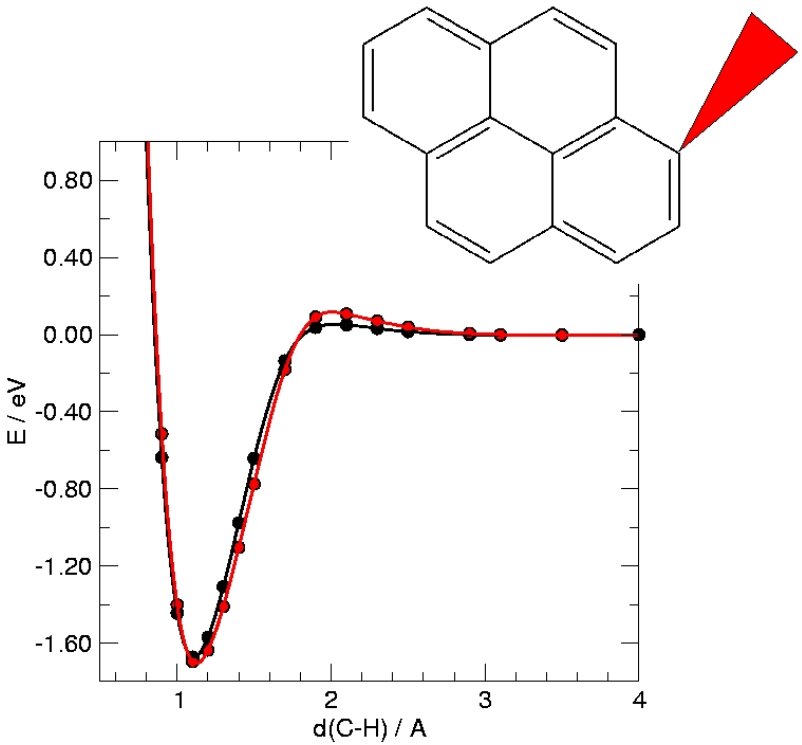

Spin-density

H + Balanced PAH

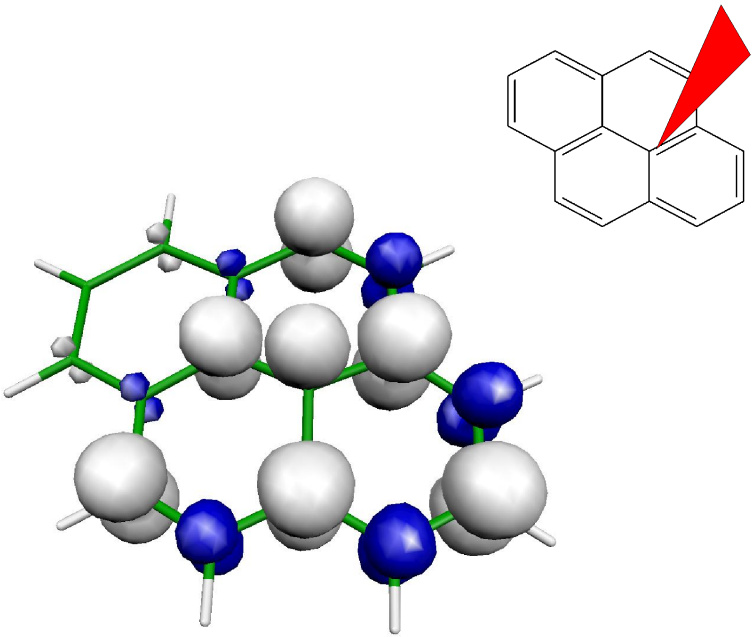

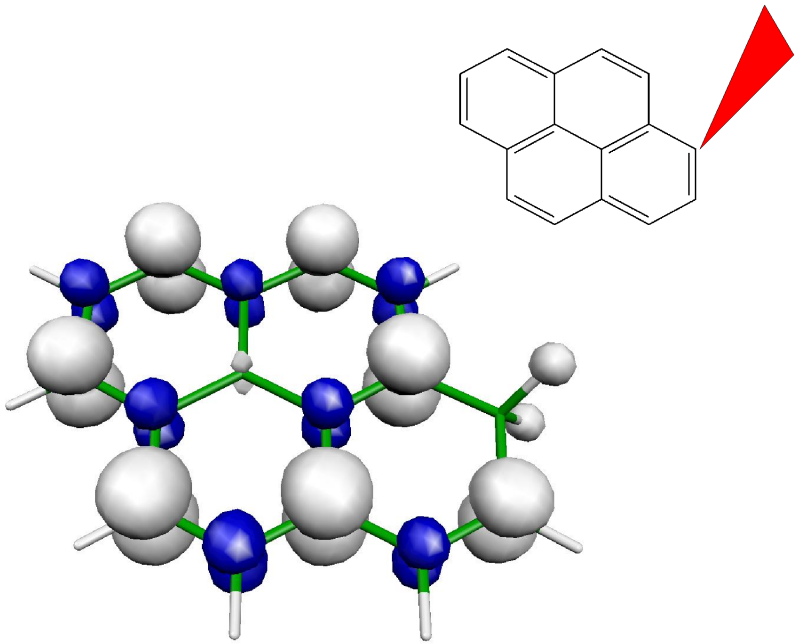

Spin-density

Imbalanced PAH

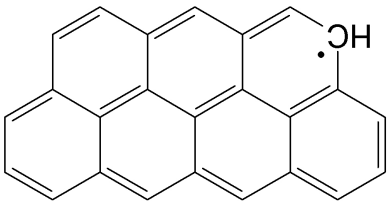

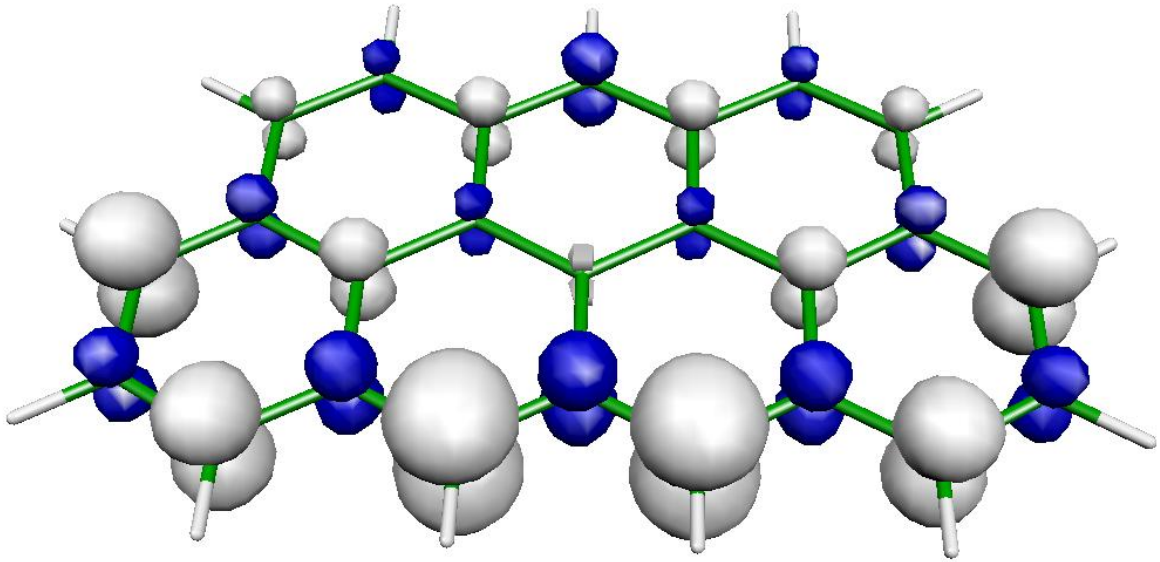

Outline

Logic applications

The need for opening a gap

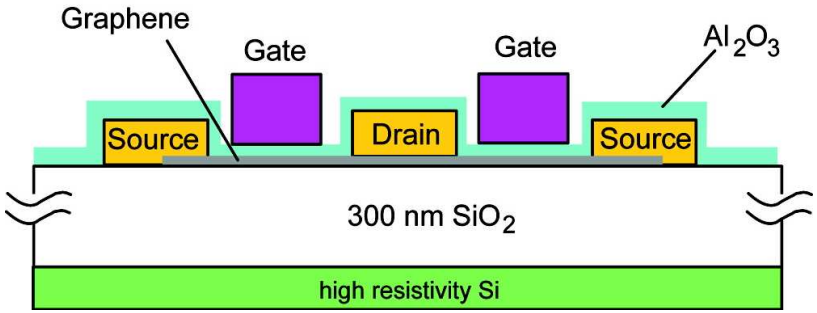

$$n_S = \epsilon_0 \epsilon \frac{V_g}{t\,e}$$

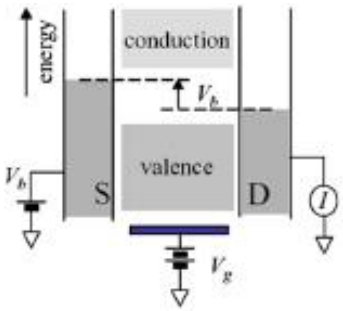

P. Avouris *et al.*, *Nat. Mat.*, 605, 2, (2007)

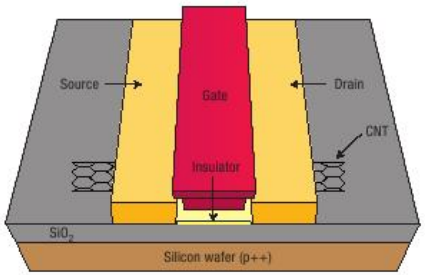

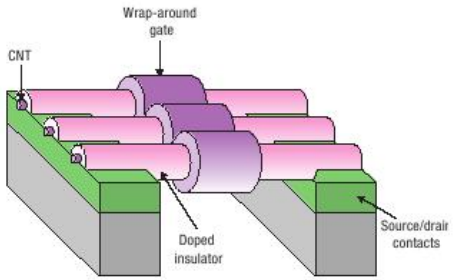

CNT-FET with ordinary and wrapped around gates

Logic applications

The need for opening a gap

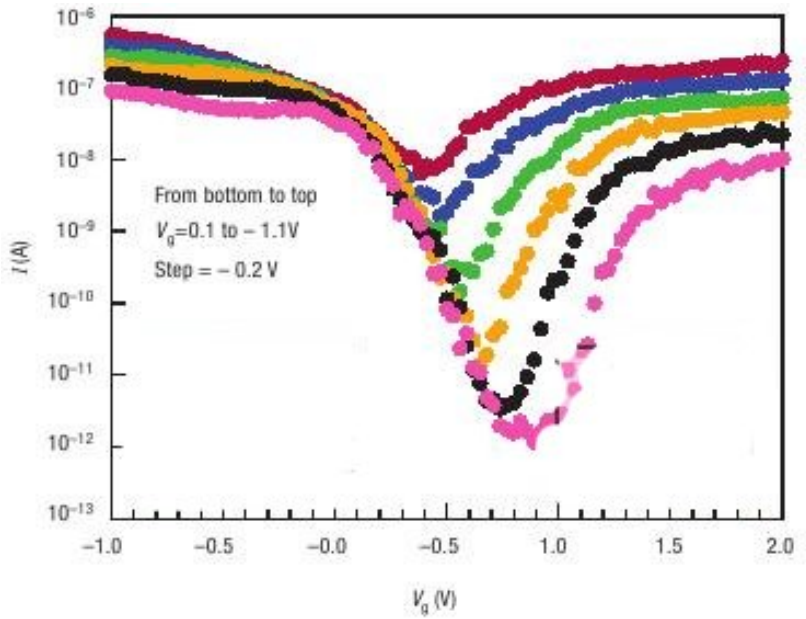

$I - V_g$ characteristics of a CNT-FET

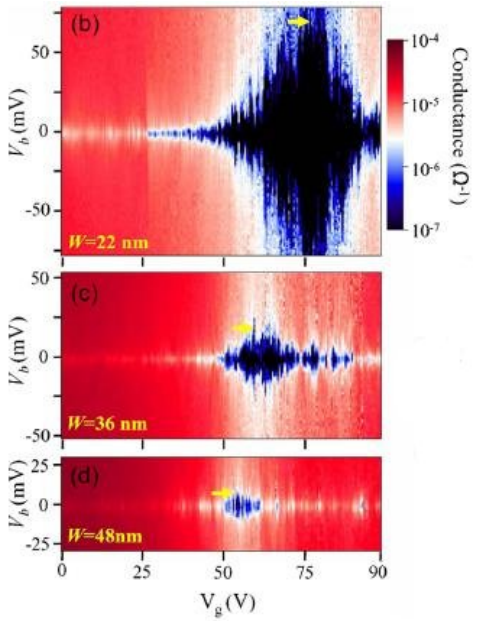

$I = I(V_g, V_{ds})$ for a 20 nm-wide GNR-FET

M. Han *et al.*, *Phys. Rev. Lett.* 98, 206805 (2007)

Logic applications

The need for opening a gap

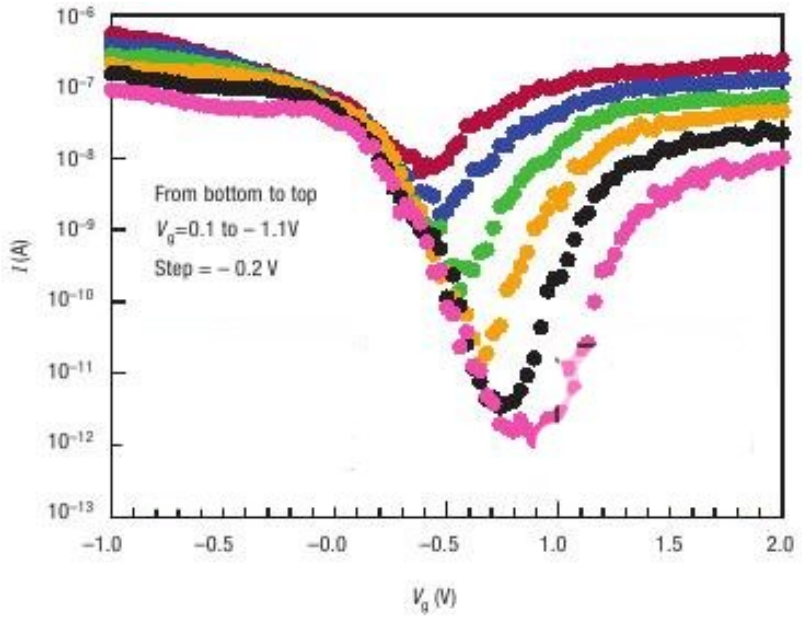

$I - V_g$ characteristics of a CNT-FET

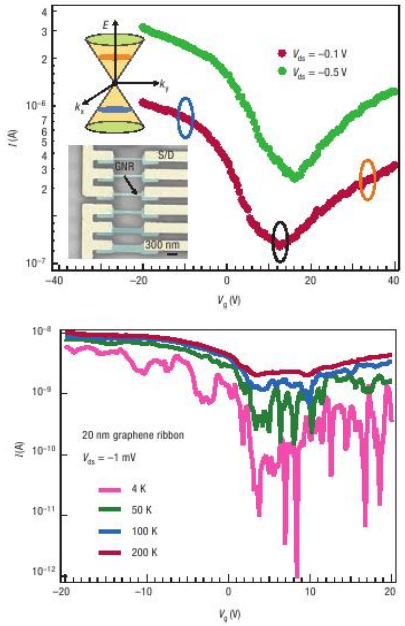

$I = I(V_g, V_{ds})$ GNR-FET

Symmetry

Why graphene is gapless?

r-space

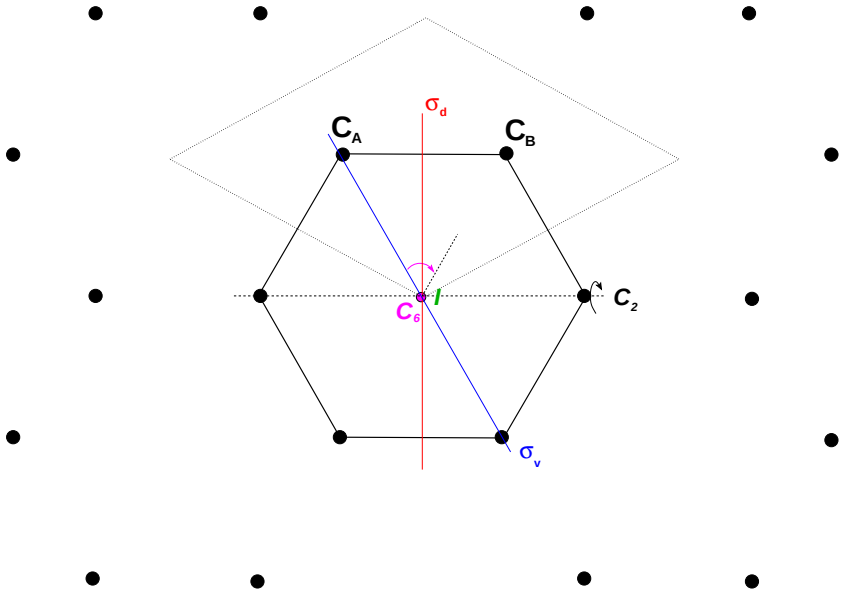

$G_0 = D_{6h}$

k-space

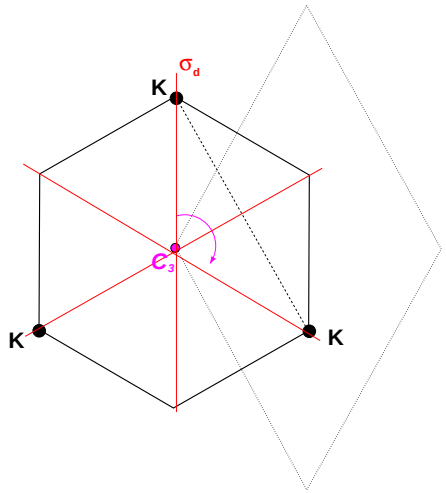

$$G(\mathbf{k}) = \{g \in G_0 | g\mathbf{k} = \mathbf{k} + \mathbf{G}\}$$

$$\Rightarrow G(\mathbf{K}) = D_{3h}$$

Symmetry

Why graphene is gapless?

r-space

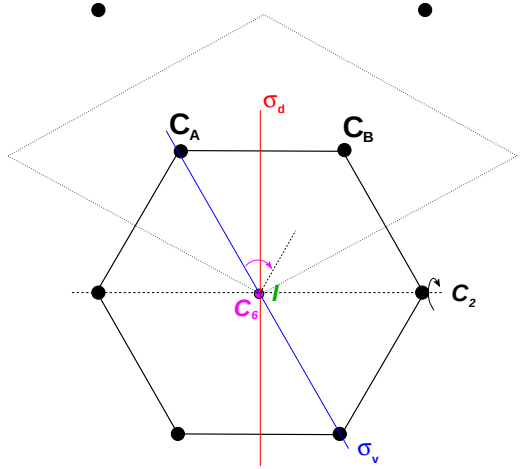

$G_0 = D_{6h}$

$$|A_{\mathbf{k}}\rangle = \frac{1}{\sqrt{N_{BK}}} \sum_{\mathbf{R}\in BK} e^{-i\mathbf{kR}} |A_{\mathbf{R}}\rangle$$
$$|B_{\mathbf{k}}\rangle = \frac{1}{\sqrt{N_{BK}}} \sum_{\mathbf{R}\in BK} e^{-i\mathbf{kR}} |B_{\mathbf{R}}\rangle$$

$$\langle r|A_{\mathbf{r}}\rangle = \phi_{p_Z}(\mathbf{r} - \mathbf{R}_A)$$

for $\mathbf{k} = \mathbf{K}$

$\{|A_{\mathbf{k}}\rangle, |B_{\mathbf{k}}\rangle\}$ span the E'' irrep of D_{3h}

Symmetry and *bipartite* lattices

Theorem

For any bipartite lattice at half-filling, if the number of E irreps is odd at a special point, there is a degeneracy at the Fermi level, i.e. $E_{gap} = 0$

Proof.

Use electron-hole symmetry □

Designing semiconducting structures

- Consider *nxn* graphene superlattices (i.e. $G = D_{6h}$): degeneracy is expected at Γ, K
- Introduce p_Z vacancies while preserving point symmetry
- Check whether it is possible to turn the number of E irreps to be even both at Γ and at K

Counting the number of *E* irreps

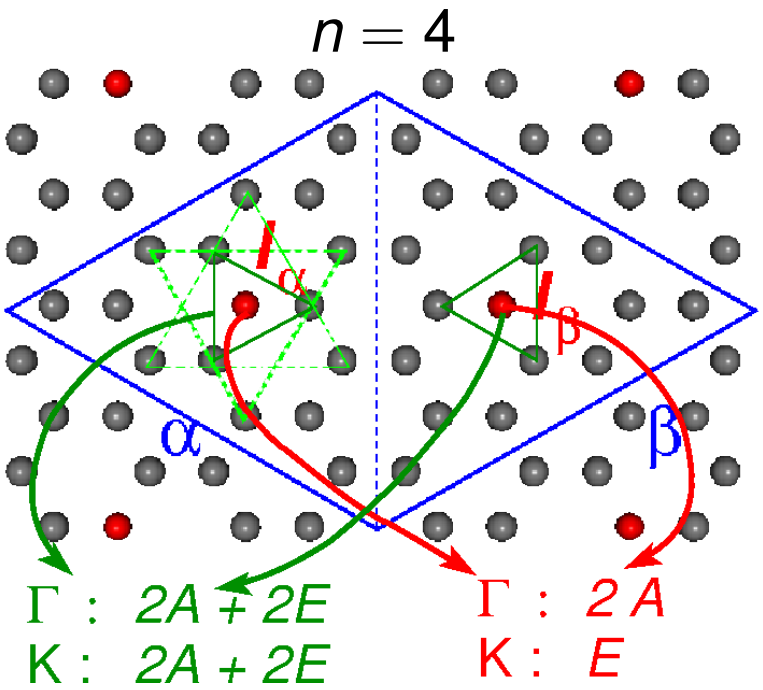

Γ	A	E
$\bar{0}_3$	$2n^2$	$2n^2$
$\bar{1}_3$	$2(3n^2+2n+1)$	$2(3n^2+2n)$
$\bar{2}_3$	$2(3n^2+4n+2)$	$2(3n^2+4n+1)$

K_n	A	E
$\bar{0}_3$	$2n^2$	$2n^2$
$\bar{1}_3$	$2n(3n+2)$	$2n(3n+2)+1$
$\bar{2}_3$	$2(3n^2+4n+1)$	$2(3n^2+4n+1)+1$

$$\Rightarrow n = 3m+1, 3m+2,\ m \in \mathbb{N}$$

(14, 0)-honeycomb

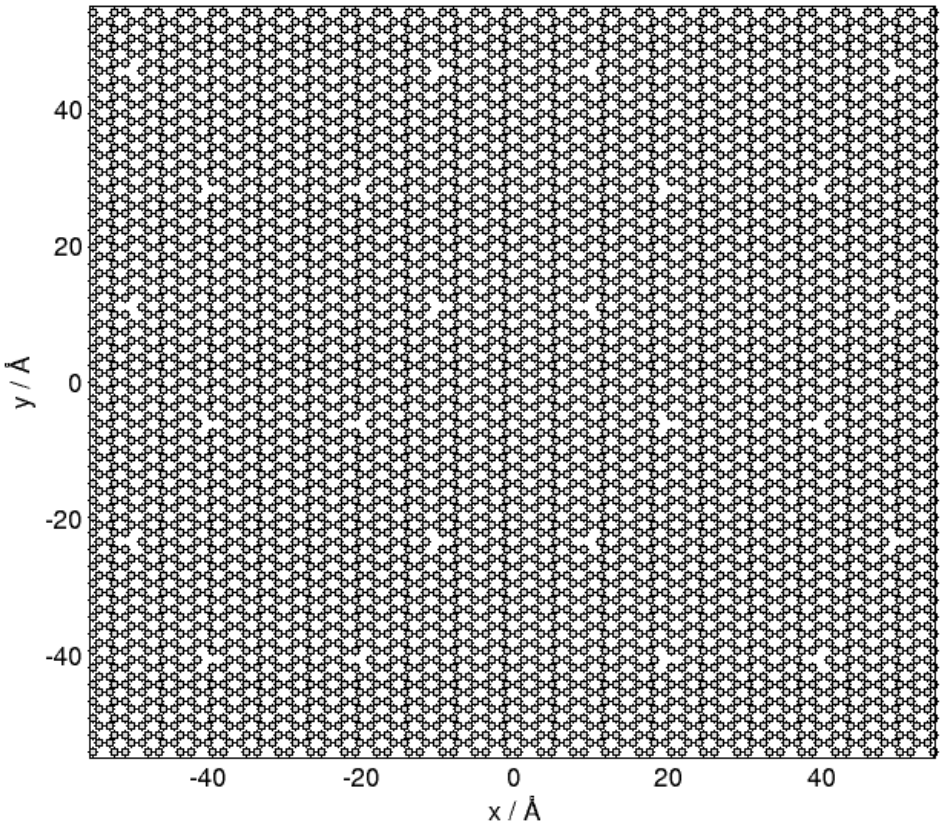

Tight-binding

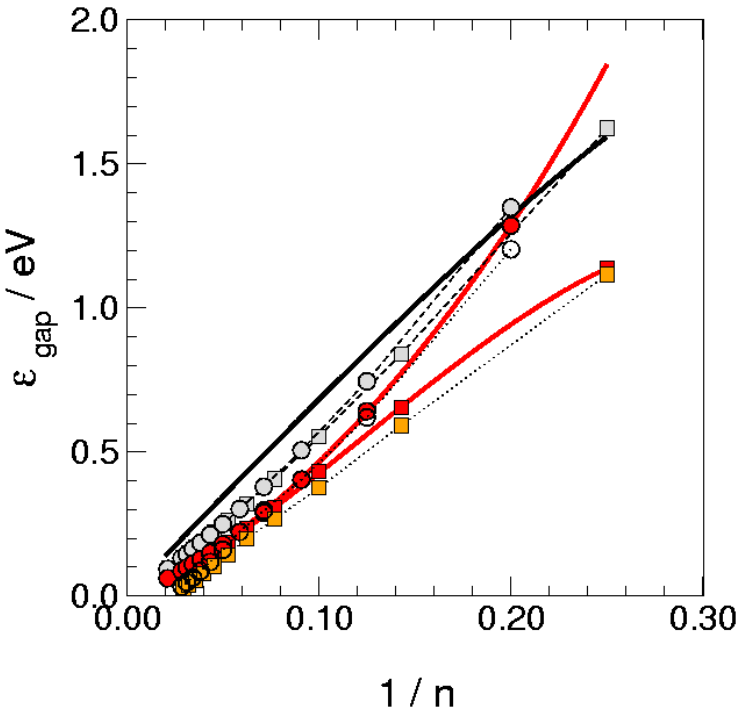

$$\epsilon_{gap}(K) \sim 2t\sqrt{1.683}/n$$

DFT

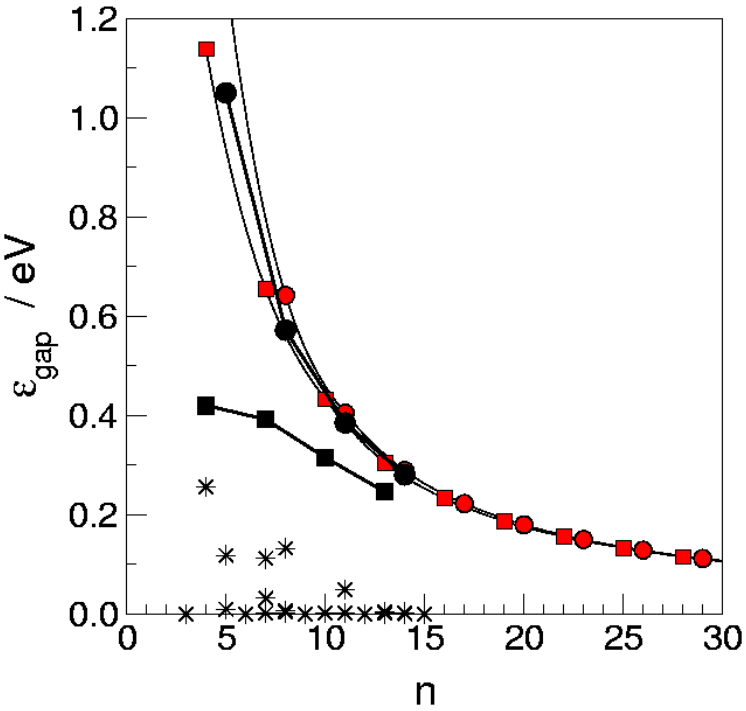

..not only: as degeneracy may still occur at $\epsilon \neq \epsilon_F$
new Dirac points are expected

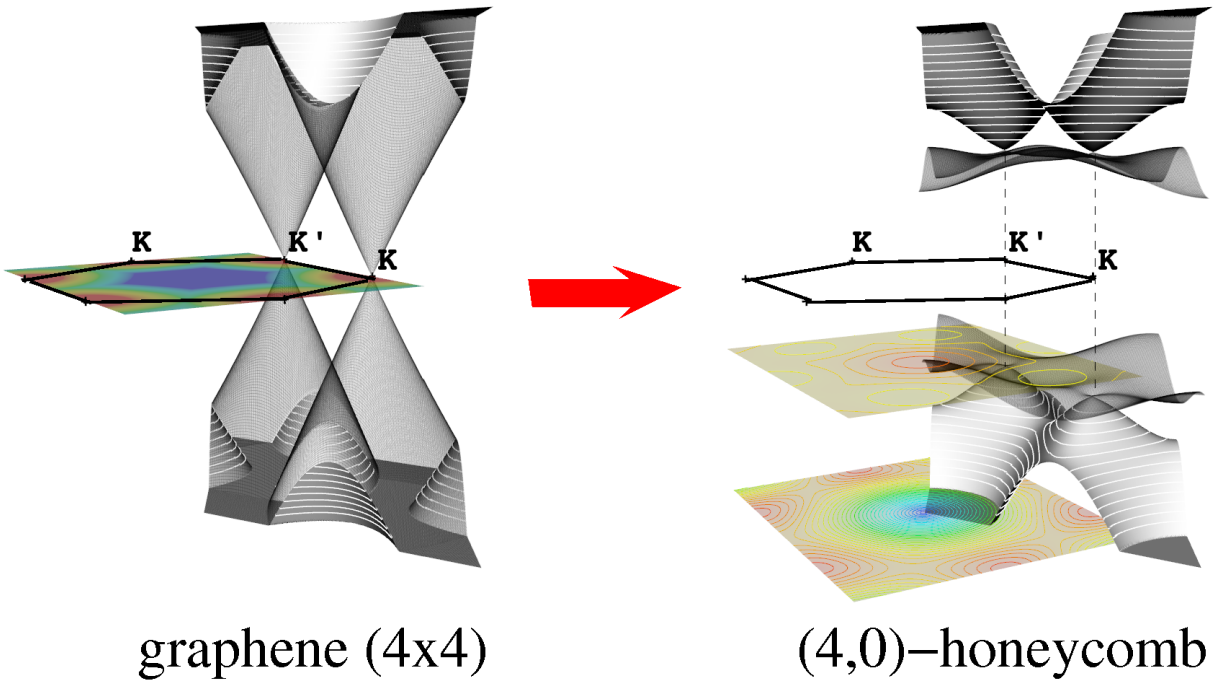

graphene (4x4) (4,0)–honeycomb

..not only: as degeneracy may still occur at $\epsilon \neq \epsilon_F$
new Dirac points are expected

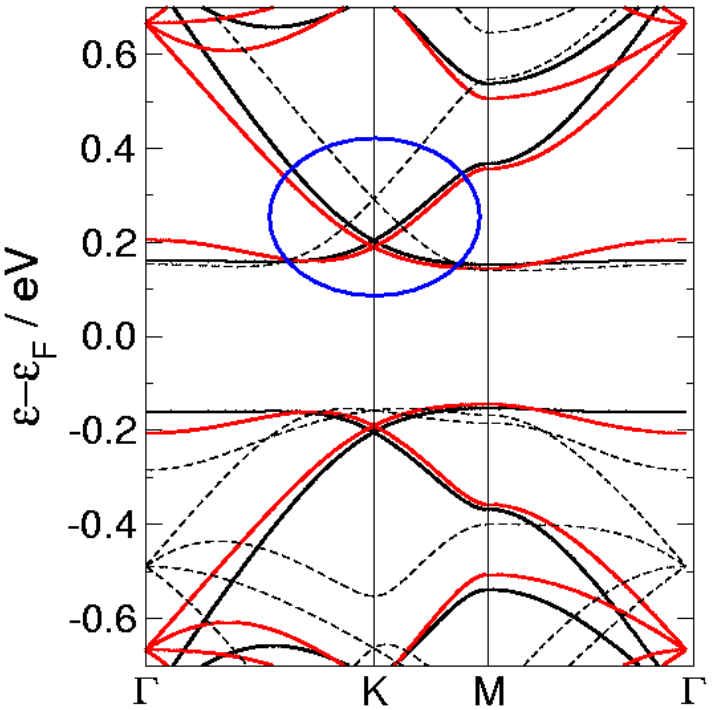

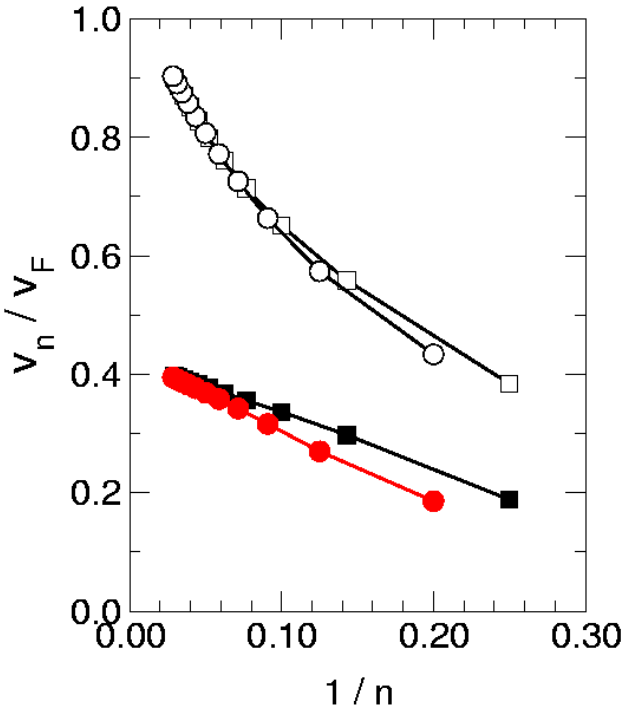

Summary

- Thermodynamically and kinetically favoured H clusters minimize sublattice imbalance
- Adsorption on magnetic C-substrates is roughly governed by spin density only
- Symmetry *breaking* is not necessary to open a gap
- New Dirac cones appears right close to the edges of the gap region

Acknowledgements

University of Milan

Gian Franco Tantardini

Simone Casolo

Matteo Bonfanti

Chemical Dynamics Theory Group

http://users.unimi.it/cdtg

University of Oslo

Ole Martin Lovvik

ISTM

Alessandro Ponti

+-x:

C.I.L.E.A. Supercomputing Center

Notur

I.S.T.M.

Acknowledgements

Thank you for your attention!